1993

A feasibility study of detached breakwater designs using a combined refraction/diffraction wave model, Virginia Beach, Virginia

John D. Boon
Virginia Institute of Marine Science

A Feasibility Study of Detached Breakwater Designs Using a Combined Refraction/Diffraction Wave Model Virginia Beach, Virginia

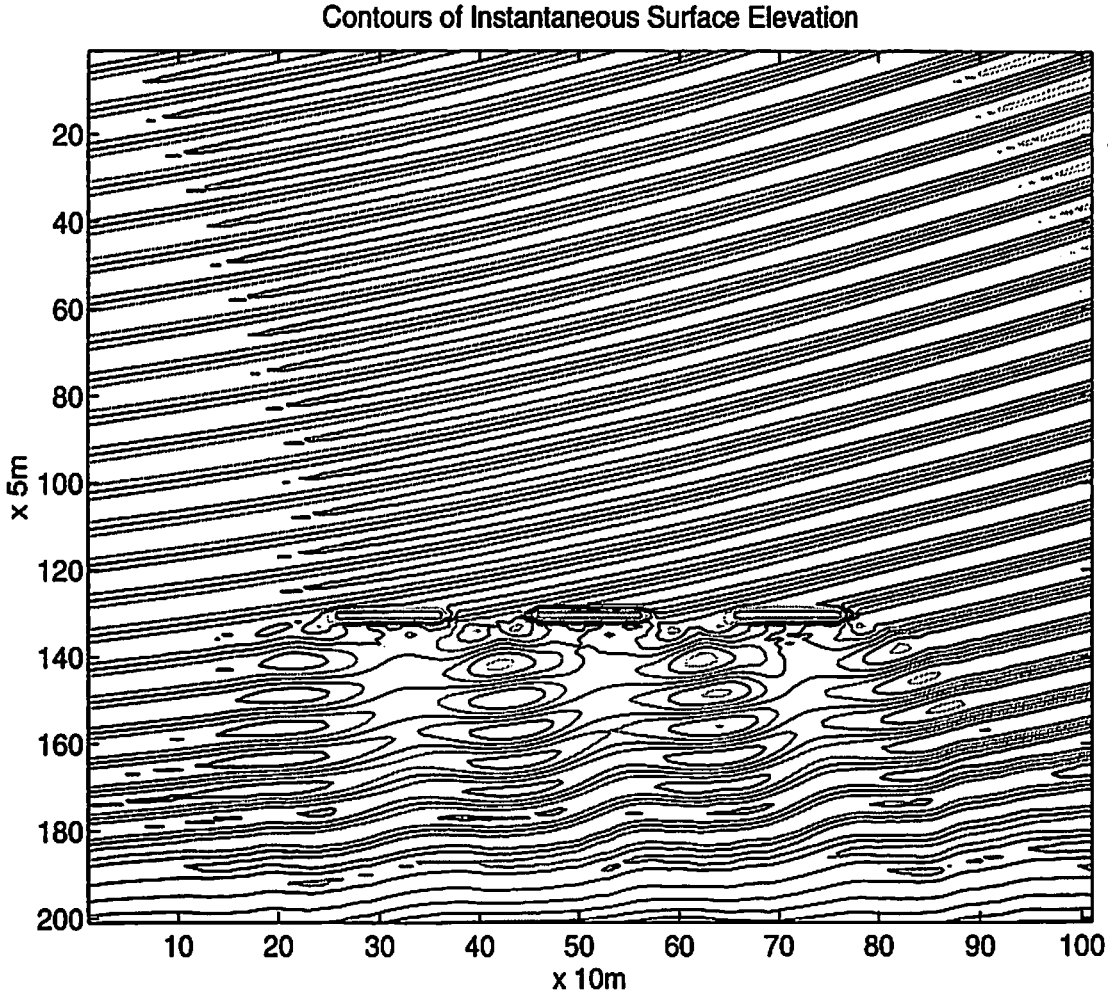

John D. Boon
School of Marine Science/Virginia Institute of Marine Science
College of William and Mary
Gloucester Point, VA 23062

Technical Report to the Virginia Department of Conservation and Recreation
Division of Soil and Water Conservation
Bureau of Rivers and Shores
October, 1993

TABLE OF CONTENTS

I. INTRODUCTION

A. Objectives - The Virginia Institute of Marine Science, together with management agencies in the Commonwealth, has a continuing interest in the matter of beach preservation along Virginia's Atlantic coastline. This interest is particularly acute along the coastline fronting the resort city of Virginia Beach, Virginia, where some 225,000 cubic meters of artificial sand nourishment are required each year to maintain recreational beaches. Wright et al.(1987), in their detailed report on beach dynamics from Cape Henry to False Cape, have stated that offshore loss of sand is a major cause of shoreline erosion in the Virginia Beach sector. Because of the narrowness and steepness of the nearshore zone in that sector, beaches are highly sensitive to offshore sand transport, a key factor in the erosion that now occurs 15% to 40% of the time. They further observed that structure-based mitigation efforts, with the structures now in use (bulkheads), are ineffective in retaining the fill placed in front of them.

As one possible alternative to costly and continuing cycles of annual maintenance that are now supported by city, state and federal programs, it has been suggested that detached breakwaters should be examined regarding their ability to 1) modify incident waves approaching the beach and 2) decrease longshore and/or offshore sand movement in selected sectors. Sometimes called segmented breakwaters when gapped, multiple units are involved, detached breakwaters are elongate, shore-parallel structures placed on the bottom whose crests rise to some specified height above the bottom or above the free surface. They have been extensively deployed in countries outside the Americas (notably Japan and Spain) where they typically consist of graded stone placed in a rubble-mound structure of trapezoidal cross-section.

Now increasingly used in the U.S., detached breakwaters have been the subject of numerous studies on shore protection methods (CERC, 1984; Dally and Pope, 1986; Suh and Dalrymple, 1987; Rosati, 1990). Rosati (1990) presents a comprehensive summary of various empirical studies on the functional design of detached breakwater systems on ocean coastlines. Within the Chesapeake Bay, Hardaway and Gunn (1991) have described twelve functioning examples of segmented breakwater systems with attached cusps (tombolos) called headland breakwaters. The latter are installed in comparatively shallow depths where they form highly stable 'pocket beaches' separated by the cusps. Unlike ocean beach systems, these structures experience short-period gravity waves of lesser amplitude within the Bay's microtidal environment that includes both Maryland and Virginia shores.

B. Detached Breakwater Design

The basic design function of a detached breakwater is to selectively reduce or alter the transmission of incident wave energy at some point seaward of the shoreline. The objective is not simply to reduce wave height at the visible shoreline (the subaerial beach face that everyone sees) but to create energy gradients starting from the shadow zone behind the breakwater. The gradient may be optimized so that sand tends to deposit in the intervening nearshore region leading to the beach. Wave diffraction may also be utilized to induce shoreline response ranging from the formation of a small cusp or **salient** to a full **tombolo** with actual shoreline attachment in the lee of the structure. Given the proper breakwater design parameters, guided by nearshore bathymetry and local wave conditions, one may select a response that is optimum for a given site. For example, a tombolo would not be the desired response where the objective is to reduce, but not eliminate, longshore sand transport through a given sub-sector to a downdrift area. This would likely be the case for most of the Virginia Beach sector.

Detached breakwaters induce beach change through a combination of wave reflection, refraction and diffraction processes as well as through turbulent wave energy dissipation controlled by the shape and permeability of the structure. For impermeable breakwaters, a key parameter is the **structure-to-distance ratio, L_s/X**, where L_s is the structure length and X is the distance from shore. The smaller the ratio, the more likely that waves diffracting around the ends of the breakwater will intersect behind the breakwater 'shadow' zone before undistorted waves reach the adjacent beach. In some cases a zone of increased wave amplitude may result that tends to inhibit tombolo formation offshore while not restricting salient development at the beach. Dally and Pope (1986) recommend $L_s/X = 0.5$ or less for single and segmented breakwaters when salient formation only is desired, recommending $L_s/X = 1.0 - 2.0$ when a tombolo is required.

To accomplish at least some of their function, detached breakwaters need not be subaerial structures. Ahrens (1984) has studied the behavior of submerged "reef" breakwaters in terms of their structural stability properties as well as their ability to reduce wave energy transmission past the structure. In effect, these breakwaters mimic the behavior of nearshore coral reefs fronting tropical lagoons. In addition to requiring less material to construct and being less costly to maintain, submerged breakwaters may have an aesthetic advantage over emergent structures interposed on natural seascapes.

The present report does not advocate that any particular form of shore protection be constructed at Virginia Beach at this time. However, it does advise the undertaking of appropriate

model studies to show the effects that various configurations of detached breakwaters might have on the existing shoreline for the sector highlighted in Figure 1 (Virginia Beach grid). This is the sector that includes the major recreational beaches of the city.

It is noted that a highly permeable metal breakwater was previously installed in the Virginia Beach sector at the 18th street location in March 1973. It was placed on the bottom at a depth of 9.8 feet (3 m) approximately 426 feet (130 m) from shore. Ludwick et al.(1975) studied its performance and reported no discernible effects (caused by the approximately 400 m length of discontinuous structure) on observed inshore wave heights, longshore currents or shoreline position during the course of a 13 month field investigation. The description given of this structure, however, bears little resemblance to the impermeable or semipermeable rubble mound or graded stone structures most commonly used in detached breakwater construction in the U.S. and abroad. In their study, Ludwick et al. (1975) made observations of wave period and breaker angle atop a tall building at the shoreline. It is significant that no mention was made of surface wave modification (i.e., diffraction patterns) occurring in the lee of the structure in question.

C. Wave Model Studies and Model Development

The previously mentioned study by Wright et al.(1987) included an intensive investigation of wave modifications over the shoreface using a modified version of **RCPWAVE**, a linear wave propagation model developed by Ebersole et al.(1986) as part of the U.S. Army Corps of Engineers Regional Coastal Processes Numerical Modeling System. Modifications were made by VIMS scientists to include energy dissipation determined by a variable wave friction factor governed by the apparent bed roughness. One of the purposes of the **RCPWAVE** model application in that study was to broadly typify the nature of shoreface wave transformation in the coastal sector extending from False Cape to Cape Henry (Figure 1). Model runs were made for three wave types beginning at a distance of 6 km from shore: 1) a normally incident modal wave from the east with 1.0 m height and 9 second period, 2) a northeast storm wave of 2.1 m height and 8 second period, 3) a normally incident design wave of 6.0 m height and 15 second period similar to recorded hurricane waves for the region (e.g., Hurricane Gloria, September, 1985). Each of these runs, when including the effects of frictional attenuation, predicted greater breaking wave heights in the vicinity of Sandbridge, Virginia, located in the southern sector of the region, as compared to the northern sector including the resort strip of Virginia Beach. The shoreface profile off Sandbridge is comparatively steep so that incoming waves experience less frictional attenuation there than at Virginia Beach where the shoreface contains a broad shoal area (Figure 1).

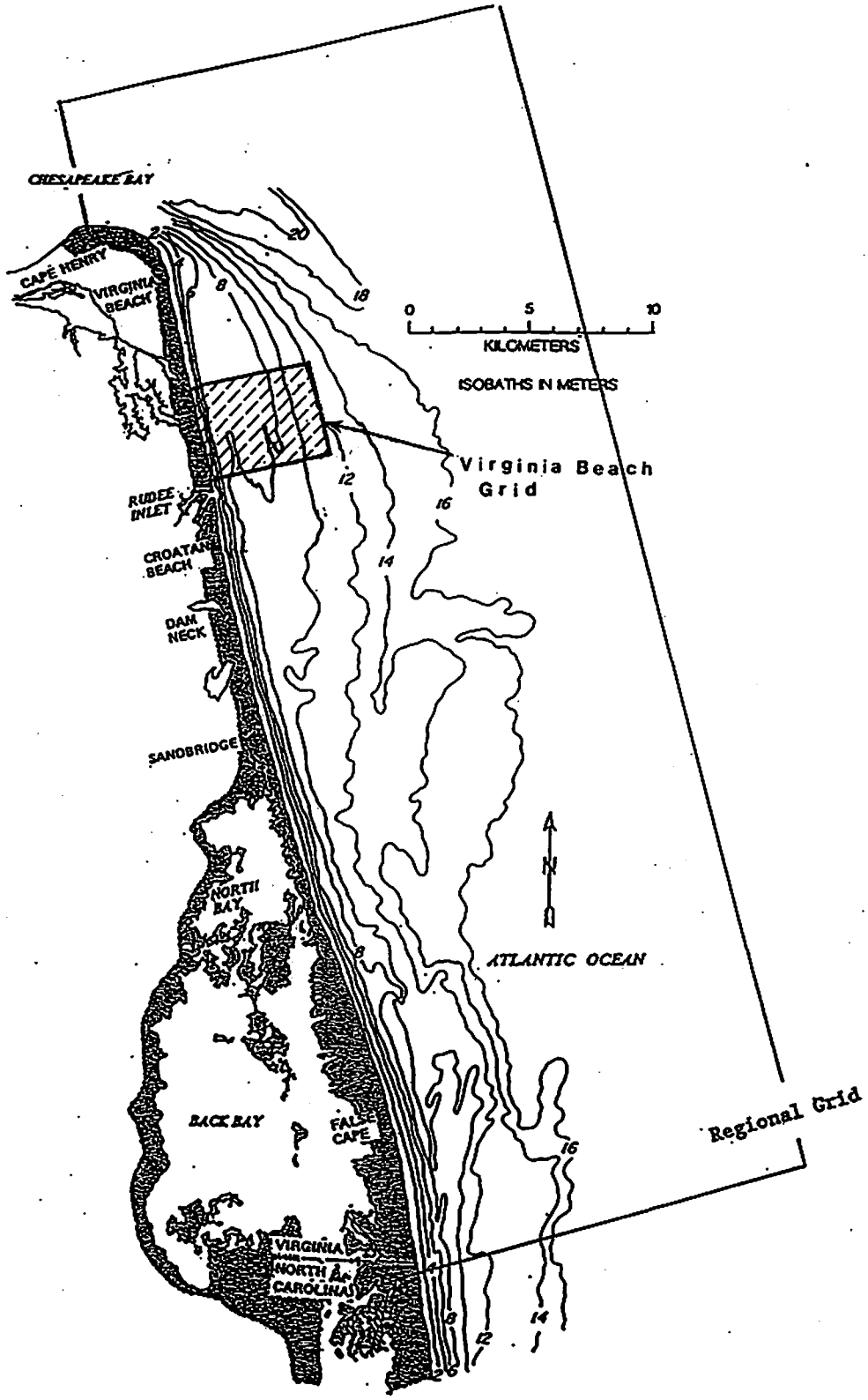

Figure 1. Location map showing the Virginia Beach Grid.

RCPWAVE is a numerical model specifically developed to predict coastal wave processes on a regional scale. Although it includes both wave refraction and diffraction, it is a linear model that does not provide the necessary means to investigate either of these processes in shoal areas at grid intervals of ten meters or less. This is the minimum resolution needed to represent a coastal structure such as a detached breakwater.

A new combined refraction and diffraction model, **REF/DIF 1, version 2.3**, developed by Dalrymple and Kirby (1991), has been used in the present study. It permits linear or weakly nonlinear wave simulation at both regional and local scales using a subgrid feature. The subgrid is essentially a high-resolution "window" with reduced x and y grid intervals that can be placed anywhere within the main grid representing the model domain. Complex bottom bathymetry can be depicted, along with hypothetical bottom-mounted structures, through grid implementation of surfaces expressed as a subset of x,y,z coordinates. The **REF/DIF 1** model contains several other advanced features and options, including current field representations, which are not a part of the present application and are not described here. Model runs were conducted using a Sun Sparc II workstation.

II. REF/DIF 1 MODEL APPLICATION

A. Grid Development and Bathymetric Representation

Bathymetric data obtained from the National Oceanic and Atmospheric Administration, National Ocean Service, were used to construct a bottom depth grid for the Virginia Beach sector as shown in Figure 1. The most recent hydrographic soundings (depths below mean low water at specified geographic positions) for the region were first obtained as a file of xyz points from NOAA/NOS. A computer program was written by the author employing the dip-projection method and quadrant search technique (Davis, 1986) to calculate interpolated values at specified grid intervals. The program also permitted specification of the desired size, location and orientation of the grid within the soundings region. Orientation is important because **REF/DIF 1** and similar models using the parabolic approximation method usually require a grid orientation that aligns one axis of the grid with the principal direction of wave propagation. Deviations of plus or minus 30° from the principal wave direction are normally permitted during different model runs.

The resulting bathymetric grid for Virginia Beach is illustrated as a three-dimensional plot containing, as an example, three hypothetical breakwaters placed 750 m offshore (Figure 2). The line of breakwaters shown at this distance represent one of five nearshore positions selected for testing

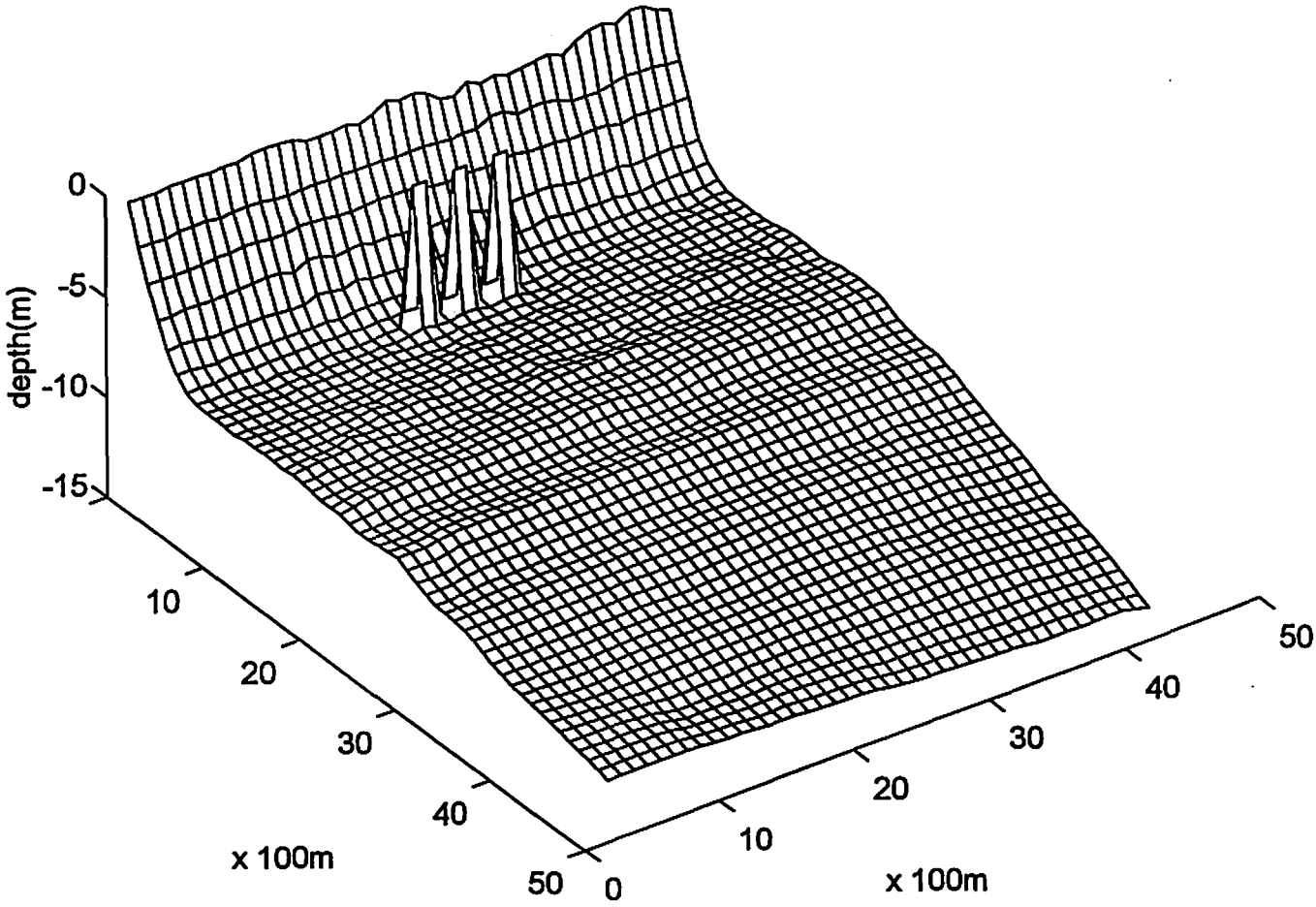

Figure 2. Bathymetry of the Virginia Beach Grid with three hypothetical breakwaters located 750 m from shore.

with the **REF/DIF 1** model as explained below.

The mesh spacing shown in Figure 2 is exactly 100 m in both the onshore and offshore directions, the total grid dimensions being 5000 m shore-normal and 4000 m shore-parallel. The bathymetry depicted shows a typical trend of increasing depths offshore but at a lesser rate than seen at other sectors such as Sandbridge (Figure 1). Figure 3 shows the actual coordinates used in model runs with the Virginia Beach Grid. The origin is located offshore in the northeast corner of the grid and the shoreline is reached at the maximum X coordinate (X=5000 m).

A sharp landward decrease in bottom depths occurs near the 8 m depth contour beginning about 700 m from shore (Figure 2). This point marks the beginning of the nearshore zone whose steep gradient, as remarked by Wright et al. (1987, p.109), is likely to be an important factor sustaining the seaward loss of beach sand. From this point seaward, bottom depths remain almost unchanged or even decrease slightly until reaching a distance of about 2500 m offshore, beyond which there is a steady increase until the maximum grid depths are reached (depths approaching 13 m in the northeast corner).

A nearshore subgrid was selected covering one square km as shown in Figures 3 and 4. For this sector, a subgrid spacing of 5 m was chosen in the X (onshore) direction while a 10 m spacing was selected for the Y (shore-parallel) direction where depth variation is least.

In the test configuration used, three submerged breakwaters were established as shown in Figure 4, with a standard 100 m crest length and 100 m gaps between lengths. In general, detached breakwater lengths should approximate the wavelength of the longest period waves normally anticipated at the site. Breakwater lengths much shorter than this will have limited influence on these waves. Ocean swell of 14 s period are near the upper limit for Virginia Beach and these have a wavelength slightly more than 100 m at a depth of 6 m. This is a length typically employed in nearshore regions although other lengths could be used as well. Detail drawings in Figure 4 illustrate the basic breakwater cross-section featuring a crest 5 m wide and a fixed base width of 25 m. Model runs were conducted using a breakwater crest depth of either zero or 1 m at one of five distances inshore (150, 250 and 350 m from land) and offshore (550 m and 750 m from land). The intermediate distance of 350 m places the design breakwaters in depths of about 6 m, or just beyond the seaward edge of the surf zone present during moderate storms.

A negative crest depth (an island or emergent shore) cannot be distinguished from a zero crest depth owing to the 'thin film' technique employed by **REF/DIF 1**; hence, a surface piercing breakwater was adopted as one of two basic breakwater types used

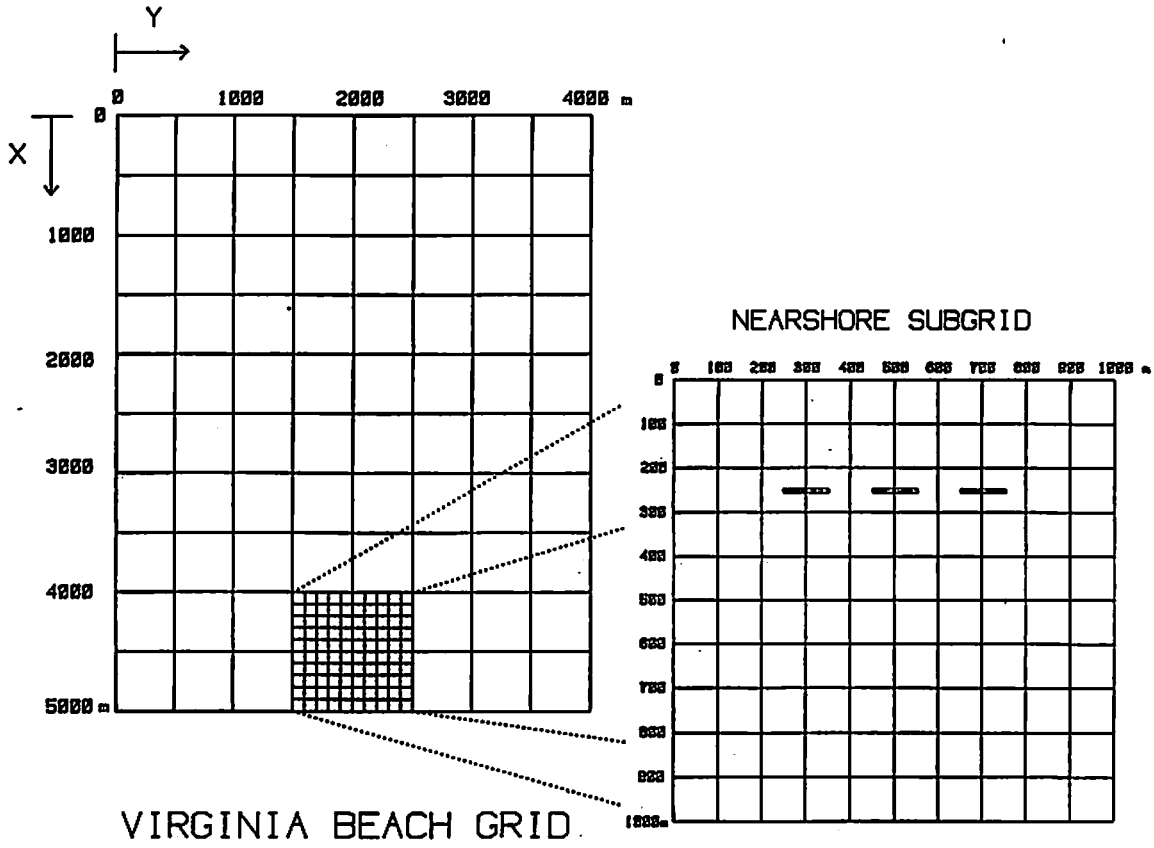

Figure 3. REF/DIF 1 model grid showing dimensions and position of the Virginia Beach Nearshore Subgrid.

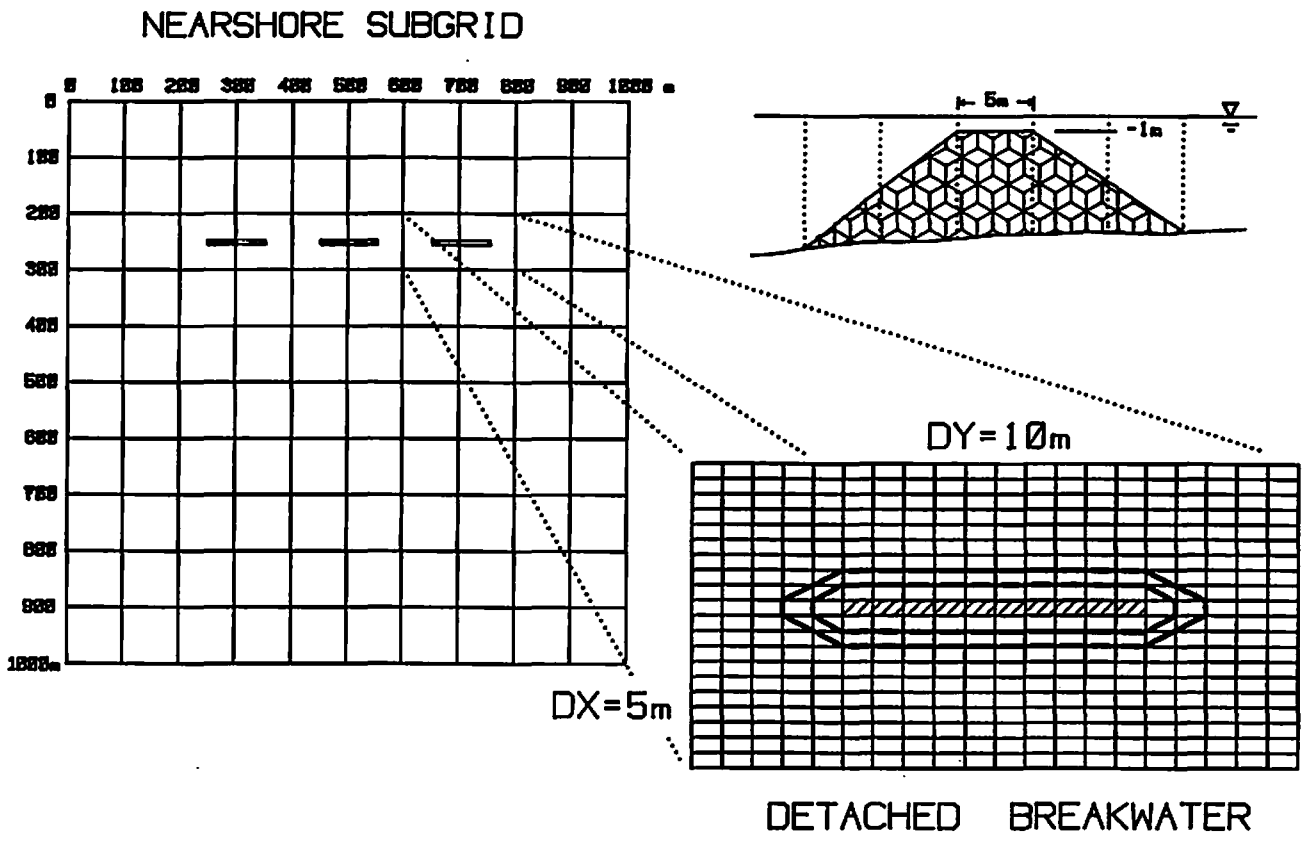

Figure 4. Virginia Beach Subgrid showing dimensions and position of detached breakwaters within user-defined subgrid blocks.

in model runs in this study, a submerged breakwater with 1 m crest depth being the other. Crest depths greater than 1 m appear to have little effect in attenuating most waves in the depth zone tested and therefore were not examined. The REF/DIF 1 model boundary conditions employed permit wave reflection from lateral boundaries (which were chosen well away from the test subgrid) but do not involve any wave reflection from down-wave structures or the shoreline.

B. Offshore Wave Characteristics and Wave Propagation

Sand mobilization in the nearshore zone is dependent on wave energy transmitted especially by the higher waves experienced during storms. Wave spectrum analysis suggests that the peak frequency of the highest waves occurring offshore during a particular storm event may not correspond to the peak frequency of the highest waves occurring inshore during the same event. The difference can occur through wave shoaling, wave refraction, frequency-dependent frictional attenuation and wave-wave interaction as component waves propagate in various directions across the shoreface. Ideally, one should input the directional spectrum of a set of storm-generated waves into a model that to simulates observed wave behavior over the inner shoreface. The lack of directional information at the outer boundary of the region (depths of 20 m or less) precludes that option here, although REF/DIF 1 has an option that generates a set of waves having a simulated directional spectrum.

Given the preliminary nature of the Virginia Beach detached breakwater investigation, discrete monochromatic waves were used exclusively in the present study, consisting mostly of waves approaching from the east. A compilation of non-directional wave data was made using information supplied by the National Oceanographic Data Center for the Chesapeake Light Tower (station CHLV2) located approximately 25 km east of Virginia Beach. The Chesapeake Light Tower is situated atop a 12 m shoal surrounded by 15 to 18 m depths below MLW datum, reaching 20 m depths before decreasing again towards shore.

Table 1 contains the numerical distribution of significant wave height (m) versus peak spectral wave period (s) for the period 2/01/85 to 6/30/91 at station CHLV2. In evaluating wave interaction with the hypothetical breakwater structures used in this study, both wave height and wave length (wave period) were considered to be key variables. Accordingly, a range of these values was selected for model runs. From Table 1, using the top value in each class interval shown, eight wave periods ranging from 6.0 s to 18.0 s were chosen and paired with the corresponding largest wave amplitudes (taken as one-half the significant wave height) that have occurred with an average annual frequency greater than 2 (i.e., more than twelve times in 6 years). These will be referred to as class extreme waves.

Table 1. Joint distribution of Significant Wave Height and Peak Spectral Wave Period at Wave Station CHLV2.

Start date = 02/01/85
End date = 12/31/92
No. data = 50215

Hmo Wave Height (m)	Peak Spectral Wave Period (s) 0 2	2 4	4 6	6 8	8 10	10 12	12 14	14 16	16 18	18 20
0.0-0.2:	0	4	0	1	4	1	0	0	0	0
0.2-0.4:	0	115	166	314	1013	160	123	70	14	0
0.4-0.6:	0	886	1286	1774	4064	769	477	262	57	1
0.6-0.8:	0	1218	2320	2387	4132	910	356	213	63	13
0.8-1.0:	0	694	2595	2116	2677	650	282	78	87	2
1.0-1.2:	0	262	1961	1593	1490	469	225	28	5	0
1.2-1.4:	0	39	1371	1125	885	326	203	45	1	0
1.4-1.6:	0	7	840	759	569	191	133	34	1	0
1.6-1.8:	0	2	515	610	350	143	86	29	1	1
1.8-2.0:	0	0	237	434	222	86	62	14	0	0
2.0-2.2:	0	1	111	281	185	77	62	11	0	0
2.2-2.4:	0	1	47	197	130	47	27	15	3	0
2.4-2.6:	0	0	18	139	93	29	22	7	2	0
2.6-2.8:	0	0	6	99	49	22	33	16	2	0
2.8-3.0:	0	0	1	92	48	31	28	12	6	0
3.0-3.2:	0	0	0	46	49	17	16	12	5	0
3.2-3.4:	0	0	2	32	39	16	8	8	6	0
3.4-3.6:	0	0	0	19	35	6	5	3	0	0
3.6-3.8:	0	0	0	17	49	11	1	3	2	2
3.8-4.0:	0	0	0	6	37	7	2	0	1	1
4.0-4.2:	0	0	0	3	31	4	1	1	0	1
4.2-4.4:	0	0	0	1	19	2	2	1	0	0
4.4-4.6:	0	0	0	0	10	2	0	0	0	0
4.6-4.8:	0	0	0	0	2	1	0	3	0	0
4.8-5.0:	0	0	0	0	1	2	2	1	1	0
5.0-5.2:	0	0	0	0	0	0	0	0	1	0
5.2-5.4:	0	0	0	0	0	0	0	0	0	0
5.4-5.6:	0	0	0	0	0	0	0	0	0	0
5.6-5.8:	0	0	0	0	0	0	0	0	0	0
5.8-6.0:	0	0	0	0	0	0	0	0	1	0
6.0-6.2:	0	0	0	0	0	0	0	0	0	0
6.2-6.4:	0	0	0	0	0	0	0	0	0	1
6.4-6.6:	0	0	0	0	0	0	0	0	0	0
6.6-6.8:	0	0	0	0	0	0	0	0	0	0

Tests were also conducted based on the most extreme wave listed in Table 1 as well as a modal storm wave of 1.0 m amplitude and 10 s period. The extremal wave was taken as having a period of 20 s and an amplitude of 3.0 m which is exceptionally rare. This corresponds to the extreme waves reported during the 1991 Halloween storm for a waverider buoy maintained at the 17 m depth at Duck, N.C. (CERC data report, U.S. Army Engineers Field Research Facility).

C. Implementation of REF/DIF 1 Wave Model Runs

Each model run began using a set of discrete wave parameters (amplitude, period and direction) specified for row 1 (X=0) at the offshore end of the Virginia Beach grid (Figure 3). **REF/DIF 1** then advanced the wave solution forward one row at a time in the X direction, calculating complex wave amplitudes (wave amplitude and phase) at each grid point along a row (Y direction). An option was chosen that allowed variable grid subdivisions (depths between rows) to be automatically calculated by the program as needed. A fixed number of interpolations was specified between columns.

The program was set to run in two stages, the first stage advancing only to row 41 (X=4000m) where the program stopped after storing the complex wave amplitudes for that row. Using another of its options, **REF/DIF 1** was then started again reading the stored amplitudes as input for a second stage run propagating waves from row 41 to row 51 at the shoreline. In this way, several nearshore 'stage two' runs could be conducted for the purpose of testing different nearshore subgrids, without having to repeat the calculations of stage one offshore. All nearshore runs in stage two employed fixed grid intervals of 5 m in the X direction and 10 m in the Y direction.

Most of the wave runs conducted specified a wave direction of 0° relative to an initial wave advance in the X direction, starting from row 1 and running approximately to the west. Other runs were made using relative offshore wave directions of +30° (advancing southwest) and -30° (advancing northwest).

Each offshore run (stage one) was made using frictional dissipation based on the turbulent bottom boundary layer option provided by **REF/DIF 1**. This option uses a linear form of the mild slope equation that includes a wave energy dissipation term, w, characterized by a Darcy-Weisbach friction factor, f, (Dean and Dalrymple, 1984). The dissipation term is calculated as

$$w = \frac{2\sigma k f |A| (1-i)}{3\pi \sinh(2kh) \sinh(kh)}$$

where |A| is the absolute value of the complex wave amplitude, σ is wave frequency, $k = 2\pi/L$ is the wave number (L = wavelength) and h is water depth. In implementing the dissipation term, a constant value of f = 0.01 was assumed. Nearshore (stage two) runs did not use the turbulent boundary layer option after initial tests produced unstable solutions (excessive amplitudes) at certain points around breakwaters placed within the subgrid area (Figure 4). Friction is most important in terms of the cumulative effect on the amplitudes of waves crossing the broader shoreface.

Figure 5 presents wave amplitudes determined for three test waves during stage one calculations using 0° initial direction for all waves. To give some idea of spatial variability in the y-direction, two lines are displayed for each combination of wave amplitude and period. These represent two shore-normal profiles, A and B, coinciding with columns Y=0 and Y=1000 m in the Virginia Beach grid (Figure 3). As seen in Figure 5, the simulated wave with maximum 3.0 m amplitude and 20 s period decreases more rapidly in the shoreward direction than either the 2.1 m (10 s) wave or the 1.5 m (14 s) wave. One of the 3.0 m runs (profile B, Y=1000m) predicts wave breaking at a distance of about 2.3 km from shore.

Comparison of the above results with corresponding data from the **RCPWAVE** runs for this sector (e.g., Figure IV-9 in Wright et al., 1987) revealed that a significantly smaller degree of wave frictional attenuation was produced using the turbulent boundary layer option in **REF/DIF 1**. This is understandable in that a different wave friction factor was used in the latter study which was not held constant but was computed such that it would be greatly increased (and probably overestimated in the Hurricane Gloria example cited by them) after considering the combined effects of movable bed roughness and bed ripples on the apparent roughness sensed by the waves. **REF/DIF 1** does not consider any frictional enhancement due to these effects and may therefore slightly overestimate nearshore wave heights predicted during moderate storms. Recently Hurricane *Emily* (a class II storm passing just offshore of Virginia Beach) produced waves with significant heights approaching 2.4 m at periods of 12-13 s approximately 1 km from shore as recorded by the US Army Engineers directional wave gage at Virginia Beach (USAE,CERC NEMO station VA01, Aug 25 - Sep 1, 1993). The corresponding wave heights at station CHLV2 are not yet available at this writing, but the data of Table 1 suggest that the waves from *Emily* were either relatively small for this type of storm, or else could be slightly overestimated assuming the predicted amplitudes of the 12-13 s class extreme waves (bottom of Figure 5) provide a valid comparison.

D. Inshore Breakwater Tests using Modal Storm Wave

Prior to conducting tests involving a range of wave conditions, a series of exploratory runs were made using detached breakwater groups positioned at varying distances from shore. For these runs, the Virginia Beach test subgrid extending 1000 m from shore was divided into an

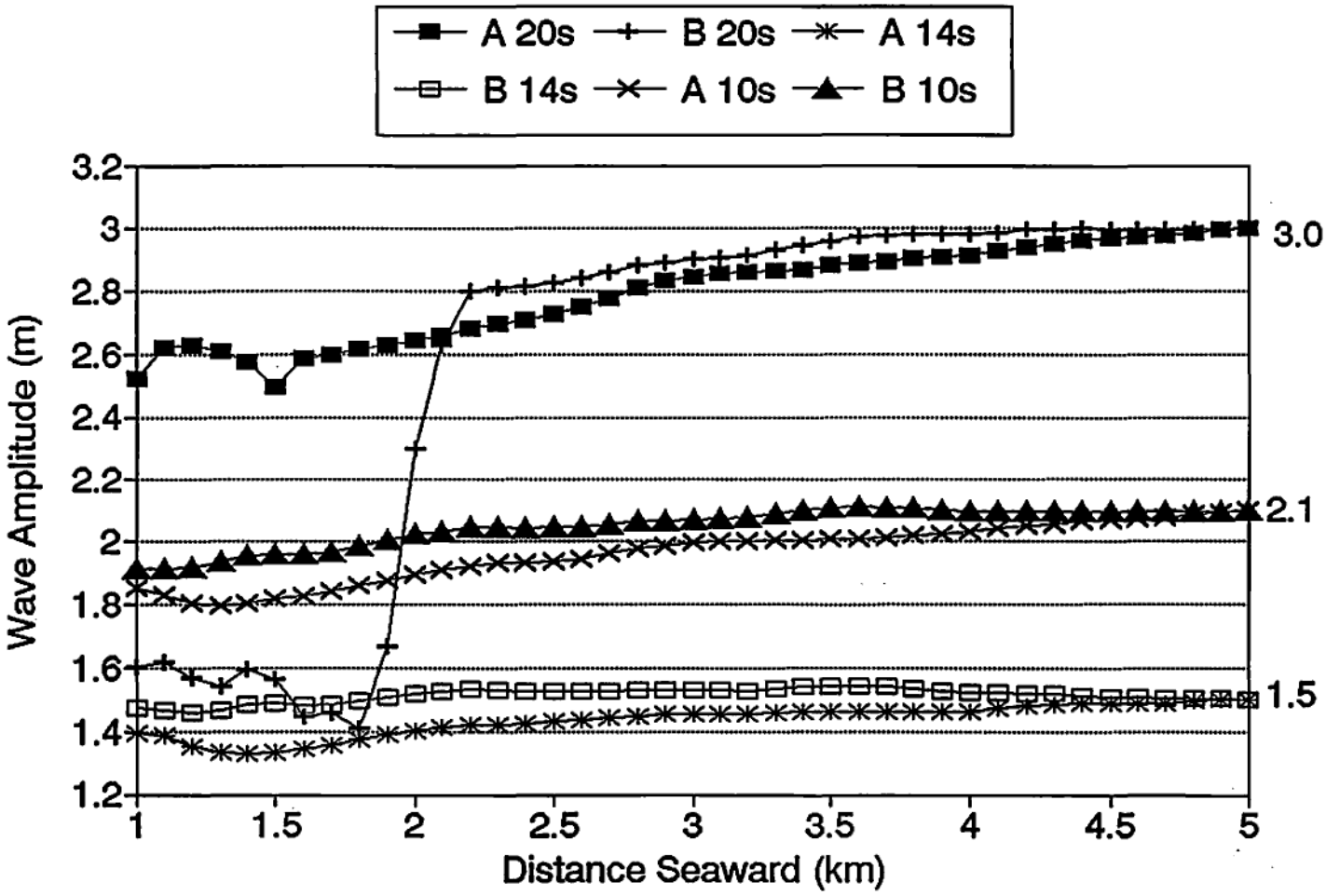

Figure 5. Predicted change in wave amplitude along profile A (Y=0) and profile B (Y=1000m) of the Virginia Beach Grid.

inshore and an offshore region. Breakwaters placed within or beyond the surf zone out to a distance of 350 m from shore were considered part of the inshore region. These tests were expected to show wave modifications that would have a high probability of direct shoreline interaction and response. Offshore tests were run specifically to investigate the amplitude reduction potential of the structures over more extensive areas beyond the surf zone. The Modal Storm Wave used in these exploratory tests was a deepwater monochromatic wave with 1.0 m amplitude and 10 s period with a relative direction of 0° (approaching from the east).

Using a standard breakwater length (100 m), the distances tested yield suitable variation in the structure-to-distance ratio which empirical evidence (e.g., Rosati, 1990) suggests will govern the type of shoreline response (salient or tombolo) one may expect. For example, the U.S. Army Engineers (CERC, 1984) recommend $Ls/X < 1$ to prevent tombolo formation.

The results of the set of nearshore runs conducted with **REF/DIF 1** are shown graphically in Figures 6 through 12. In place of the usual wave ray diagrams, contour plots of wave amplitude and water surface elevation were constructed as follows. From the raw output expressed as an array of complex wave amplitudes, $A = a + ib$, a matrix of absolute wave amplitudes $|A| = (a^2 + b^2)^{1/2}$ was computed over the subgrid domain. A contour plot of the amplitude field was then constructed using MATLAB 4.0. To convey directional sense to the wave motion, the instantaneous surface elevation was computed as $\eta = \text{atan2}(b/a)$ and similarly contoured over the subgrid.

D.1. Subgrid without Breakwaters - Contour plots for a modal storm wave run with no breakwaters installed are illustrated in Figure 6. Figure 6a shows a localized amplitude increase due to wave shoaling, from 1.0 to 1.2 m, beginning approximately 200 m from shore. Wave breaking and linear breaker height attenuation begin approximately 100 m from shore starting at the 0.8 m amplitude contour. Alternating wave crests and troughs, shown in Figure 6b, approach land in the shore-normal direction with their crest (trough) lines running parallel to the shoreline.

D.2. Single Submerged Breakwater 350 m from Shore - Figure 7 shows a single submerged breakwater with a crest depth of 1 m located 350 m from shore. Wave amplitudes and directions are again predicted based on a modal storm wave. The model predicts a moderate amount of wave amplitude reduction in the lee of the structure (from 1 m to 0.6 - 0.8 m, Fig. 7a) with a slight amplitude increase (to > 1 m) just before the breaker zone is encountered (starting at the 0.8 m line). Crest orientations (Figure 7b) illustrate the classical pattern of wave diffraction expected around the shadow zone immediately behind the breakwater crest; Predicted breaker angles, however, are only slightly changed down-wave near the 0.8 m amplitude contour. Both the predicted gradients in wave height and the opposing wave angles due to diffraction would suggest perhaps a slight tendency for shoreline salient development in line with the

breakwater, assuming the presence of an adequate sand supply. A single submerged breakwater, however, clearly would have a rather limited effect spatially in this sector.

D.3. Three Submerged Breakwaters 350 m from Shore - Figure 8 shows three submerged breakwaters, each with a crest depth of 1 m located 350 m from shore. There is an enlarged area of reduced wave amplitudes, including two low-amplitude regions (less than 0.8 m) predicted to occur down-wave and in line with the two breakwater gaps shown in Figure 8a. Three wave intersection zones (amplitude > 1 m) can also be seen in Figure 8a in line with the mid-point of the breakwaters where tombolo development would be inhibited. Weak wave crest intersections near the shoreline (Figure 8b) suggest that minor salient formation could occur but is not certain. Assuming the predictions in Figures 7a and 8a are correct, there is more than a three-fold increase in wave attenuation compared with that produced by a single breakwater. Given that expectation, three-breakwater configurations were used in all subsequent tests.

D.4. Three Surface Breakwaters 350 m from Shore - To evaluate the effect of crest depth at the 350 m distance, a run was made for three surface breakwaters with zero crest depth as shown in Figure 9. In this configuration, the zone of reduced wave amplitude is expanded in the lee of each breakwater and extends all the way to the breaker zone (Figure 9a). Unlike the previous case, there is pronounced wave amplification in the two regions down-wave from the gaps. In addition, an 'end effect' of the type described by Hardaway et al. (1993) is predicted featuring abrupt wave amplification on both flanks of the surface breakwaters. Figure 9b suggests a delayed wave diffraction pattern that should promote development of three pronounced salients at the shore in line with each breakwater. The empirical relationships previously mentioned in Rosati (1990) would suggest that no tombolo development should occur given the low structure-to-distance ratio of 100/350 = 0.29.

As previously noted, **REF/DIF 1** cannot distinguish the above configuration from that of three detached breakwaters having subaerial crests. Test runs made for a zero-height breakwater should have equal applicability for a subaerial structure with a crest height of approximately 1 m or less.

D.5. Three Submerged Breakwaters 250 m from Shore - Moving the set of breakwaters closer to shore increases the structure-to-distance ratio and the tendency to form pronounced salients. Figure 10 illustrates that a submerged breakwater group at this distance predicts roughly the same pattern of wave diffraction as the surface breakwaters 350 m from shore (Figure 9) but without the three intersection zones of enhanced wave amplitude. These now appear to have been absorbed into the breaker zone.

D.6. Three Surface Breakwaters 250 m from Shore - Figure 11 shows that surface breakwaters at the 250 m distance should produce slightly enhanced wave amplitudes relative to those of submerged breakwaters at this distance. Otherwise the degree of diffraction indicated is approximately the same except that end-effects are more pronounced.

D.7. Three Surface Breakwaters 150 m from Shore - Figure 12 depicts three breakwaters located just at the beginning of the breaker zone for the test wave of 1 m amplitude and 10 s period. A much greater degree of disturbance is indicated directly within the breaker zone and a greater degree of uncertainty among possible end-effects is also suggested. The model results and empirical data suggest that this configuration would effect a moderate to strong shoreline response that could possibly include tombolo formation.

E. Offshore Breakwater Tests using Modal Storm Wave

Figure 2. shows a three-breakwater group located 750 m from shore at the edge of the nearshore zone with its sharply increased bathymetric gradient. Obviously, the cost to construct the specified breakwaters would increase just as sharply up to this point and it is therefore important to know what advantages, if any, would be offered by locating them offshore. To explore this question, two modal storm wave runs were made at the 550 m and 750 m distance from shore (Figures 13 and 14, respectively) using submerged breakwaters with -1 m crest depth.

For the breakwater group position shown in Figure 13a, substantial wave amplitude reduction (20% - 40%) is predicted to occur over an area of approximately 0.125 km^2 or about one-quarter of the inshore area of the subgrid. The same or a slightly greater amount of reduction is indicated in Figure 14a which includes two elongate areas in line with the breakwater gaps that have more than 40% amplitude reduction. While these modifications imply little change in wave amplitude at the shoreline, they predict significant amplitude reduction over the steepest portion of the inner shoreface where long-period waves in particular can be expected to mobilize bottom sediments during storms.

Figures 13b and 14b reveal little indication of breakwater-induced modifications in wave angle for waves approaching the breaker zone. Consequently, little or no salient development would be expected for this type of offshore configuration.

F. Breakwater Tests using Selected Wave Amplitude and Period

Figures 15 - 21 contain the output for a series of model runs made using the class extreme waves from Table 1 that, as previously noted, have an annual frequency of occurrence greater than 2 and include wave periods ranging from 6.0 s to 18.0 s. Three surface breakwaters positioned 350 m offshore were tested with shore-normal waves in each run. Examining plots of wave amplitude in these figures, it is apparent that minimal end-effects can be expected given minimal period (6.0 to 8.0 s) waves. Enhanced end-effects are predicted as wave period increases from 10.0 s to 18.0 s, including pronounced wave angle distortions extending laterally well beyond the ends of the left and right breakwater. In general, waves of higher period (> 10 s) appear to produce irregular wave diffraction patterns shoreward of the breakwaters and, within the 16.0 to 18.0 s period range combined with lesser

amplitudes (Figures 20 and 21), actually predict a relative increase in wave amplitude over much of the inshore area.

G. Breakwater Tests using Maximum Wave (Halloween Storm)

Figure 22 contains the predicted wave response for the extremely long period (20 s) waves of the October 1991 'Halloween' storm which, according to observations at Duck, N.C., produced 3.0 m wave amplitudes at or near the 12 m depth contour. As previously shown in Figure 5, large amplitude waves of this kind would be expected to undergo significant frictional attenuation, and to break in some instances, when propagating across the Virginia Beach grid to within 1 km of the shore. Given large, unstable waves nearing their final approach to the shoreline, it is not surprising to see large wave reductions predicted immediately landward of the line of breakwaters where wave breaking would almost certainly occur. Figure 22 suggests that wave breaking would be tripped all along this line, including the region well beyond the ends of the left and right breakwater.

H. Breakwater Tests with Varying Wave Direction

Figures 23 - 25 show the output from model runs using a storm wave of 2.1 m amplitude and 10 s period with relative directions of +30° (Figures 23 and 25) and -30° (Figure 24) starting 5 km offshore. Looking at contours in the upper (seaward) half of each subgrid shown, one can see the effect of wave refraction which greatly reduces the incident wave amplitude as well as the angle of wave approach to the shore (from 30° to approximately 15°). In Figures 23 and 24 there are indications of three broad lobes containing further reduced wave amplitudes in the lee of the three submerged breakwaters positioned 550 m offshore. The lobes shift their position laterally by a surprisingly small distance (less than 100 m) in spite of the large change in incident wave angle (+30° to -30°) starting 5 km offshore. In Figure 25 (incident wave angle +30°) a surface breakwater group is positioned 350 m offshore where it produces strong amplitude reduction (Figure 25a) and well-developed wave diffraction patterns (Figure 25b) virtually all the way to the shoreline.

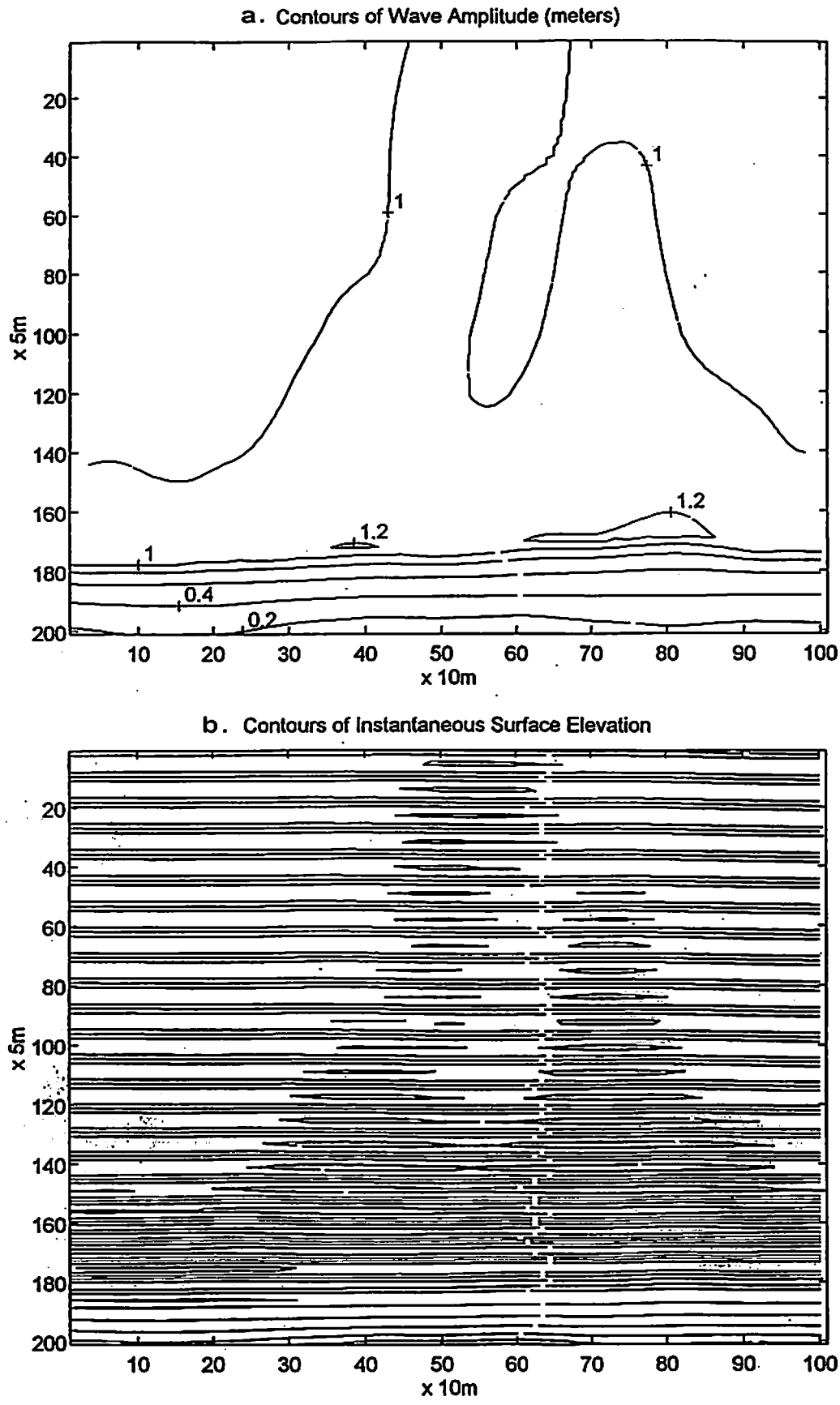

Figure 6. Wave propagation in nearshore subgrid with no breakwaters present using a modal storm wave with A = 1.0 m, T = 10.0 s, D = 0°.

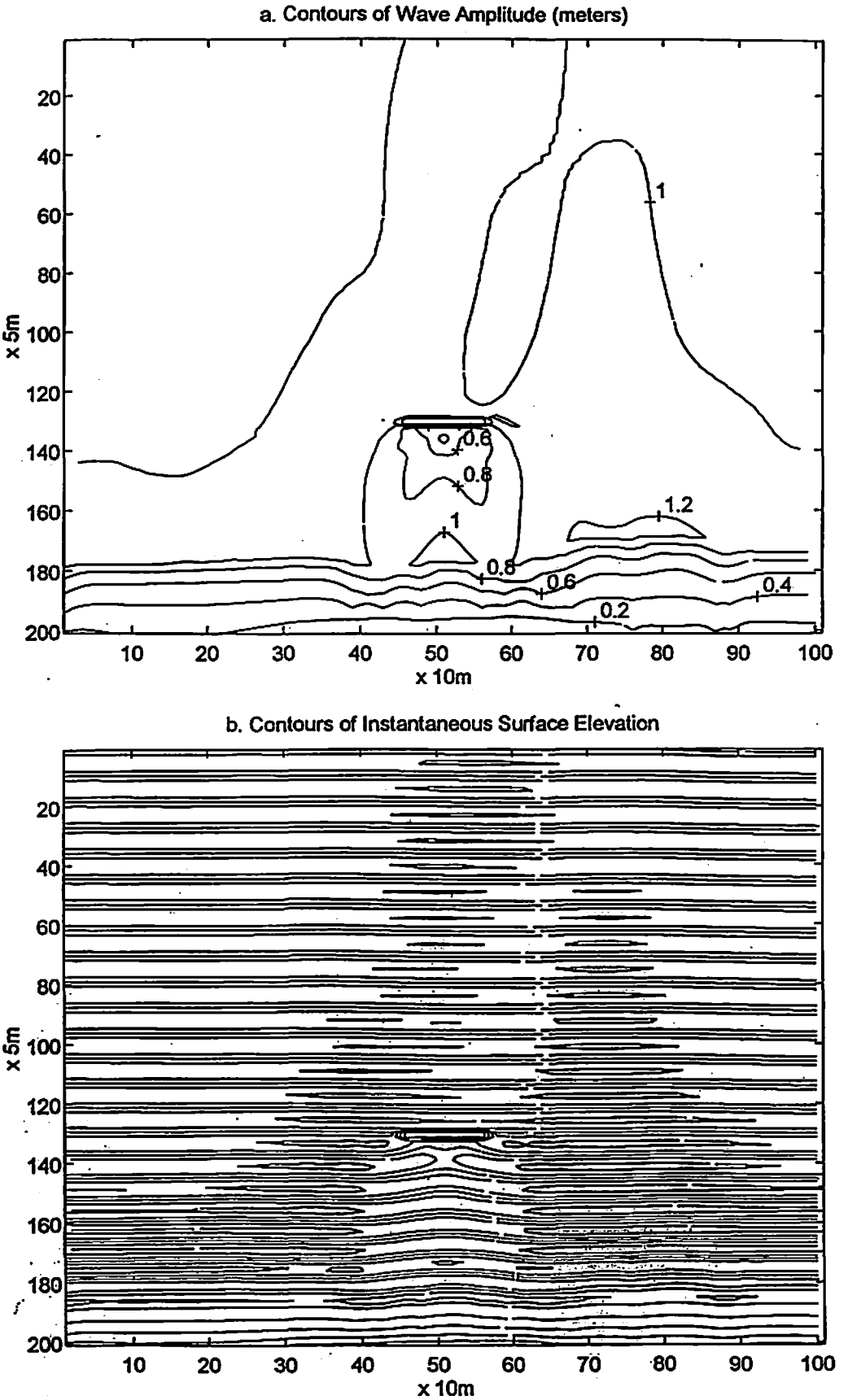

Figure 7. Wave propagation past a single submerged breakwater 350 m from shore using a modal storm wave with A = 1.0 m, T = 10.0 s, D = 0°.

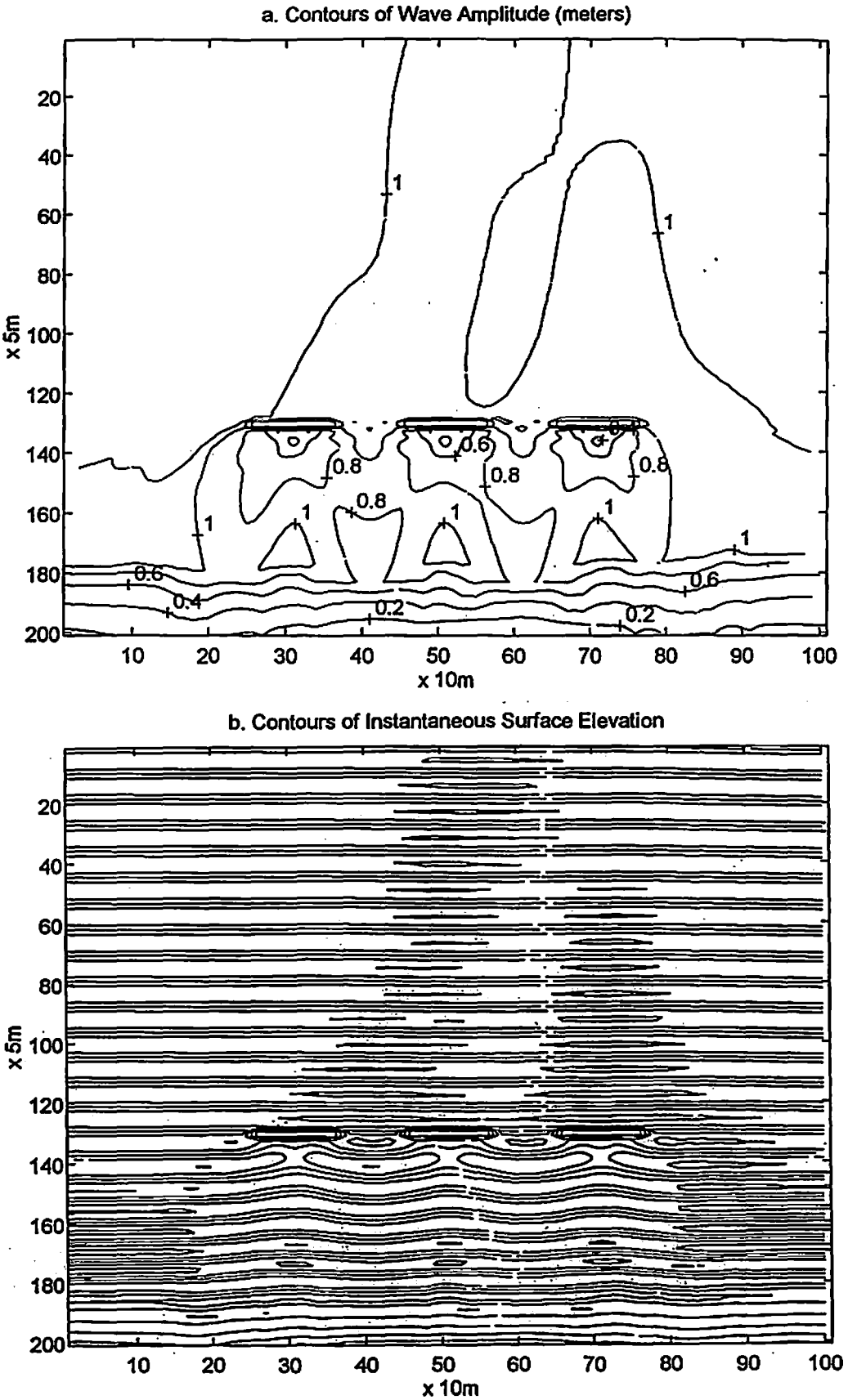

Figure 8. Wave propagation past three submerged breakwaters 350 m from shore using a modal storm wave with A = 1.0 m, T = 10.0 s, D = 0°.

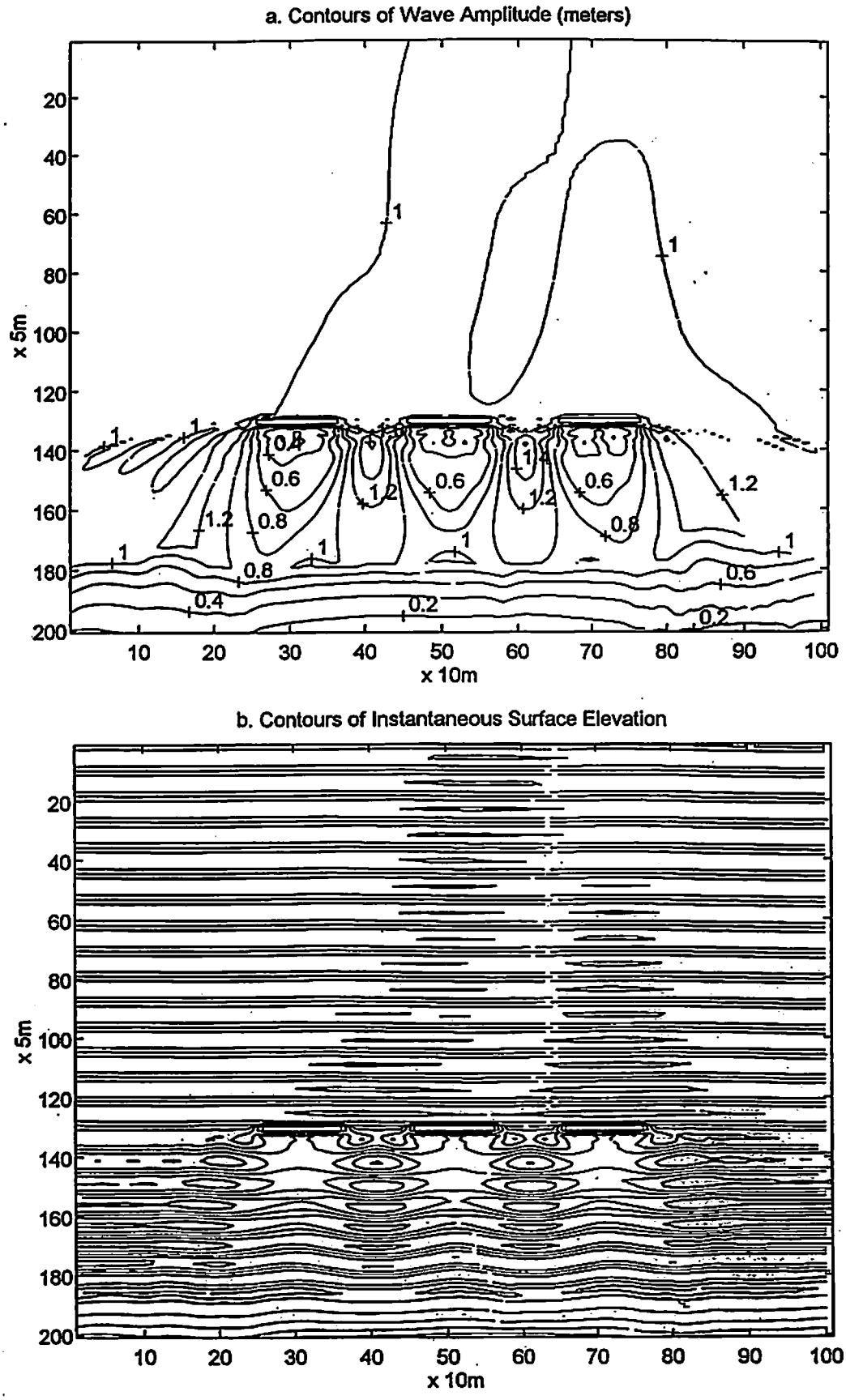

Figure 9. Wave propagation past three surface breakwaters 350 m from shore using a modal storm wave with A = 1.0 m, T = 10.0 s, D = 0°.

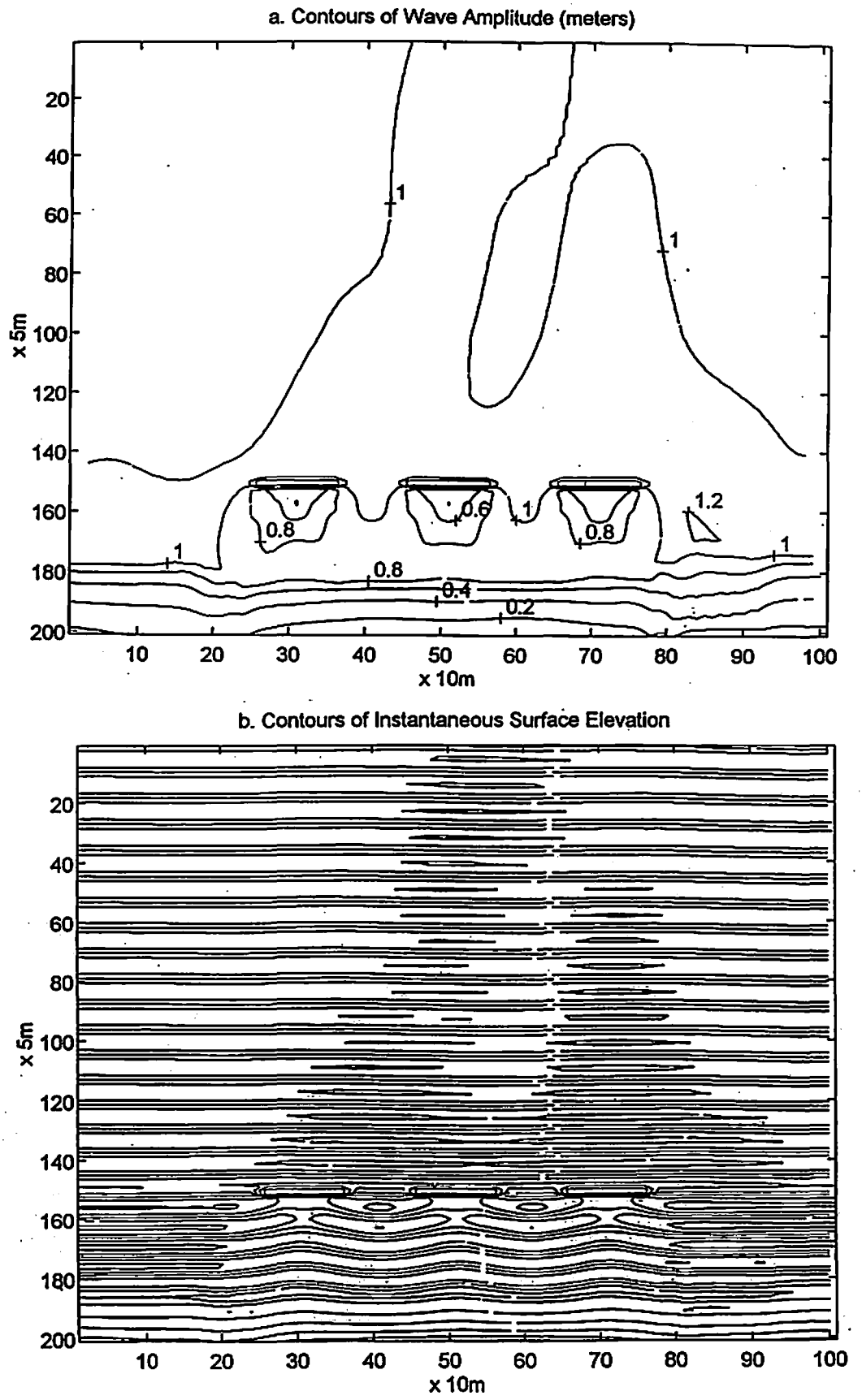

Figure 10. Wave propagation past three submerged breakwaters 250 m from shore using a modal storm wave with A = 1.0 m, T = 10.0 s, D = 0°.

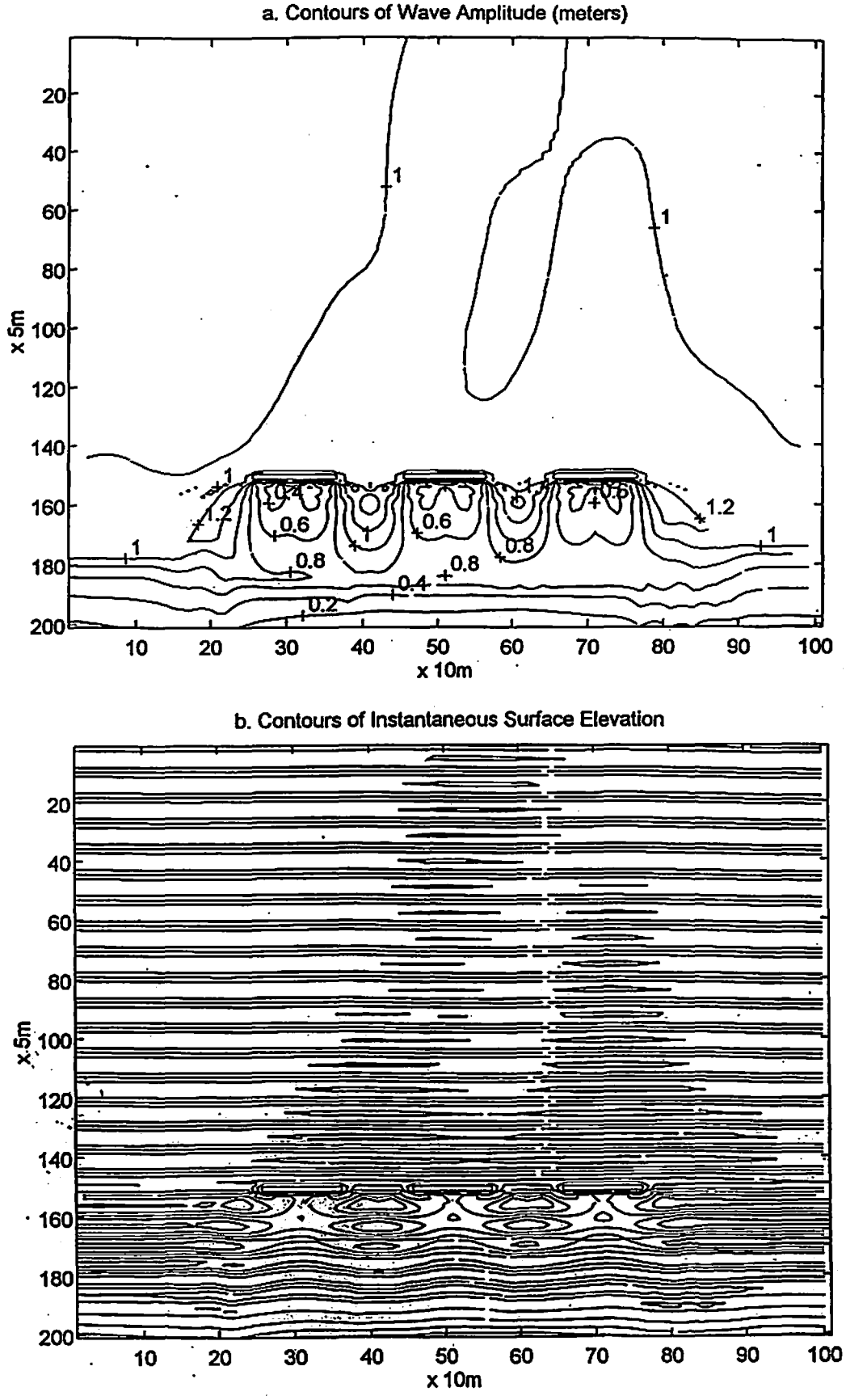

Figure 11. Wave propagation past three surface breakwaters 250 m from shore using a modal storm wave with A = 1.0 m, T = 10.0 s, D = 0°.

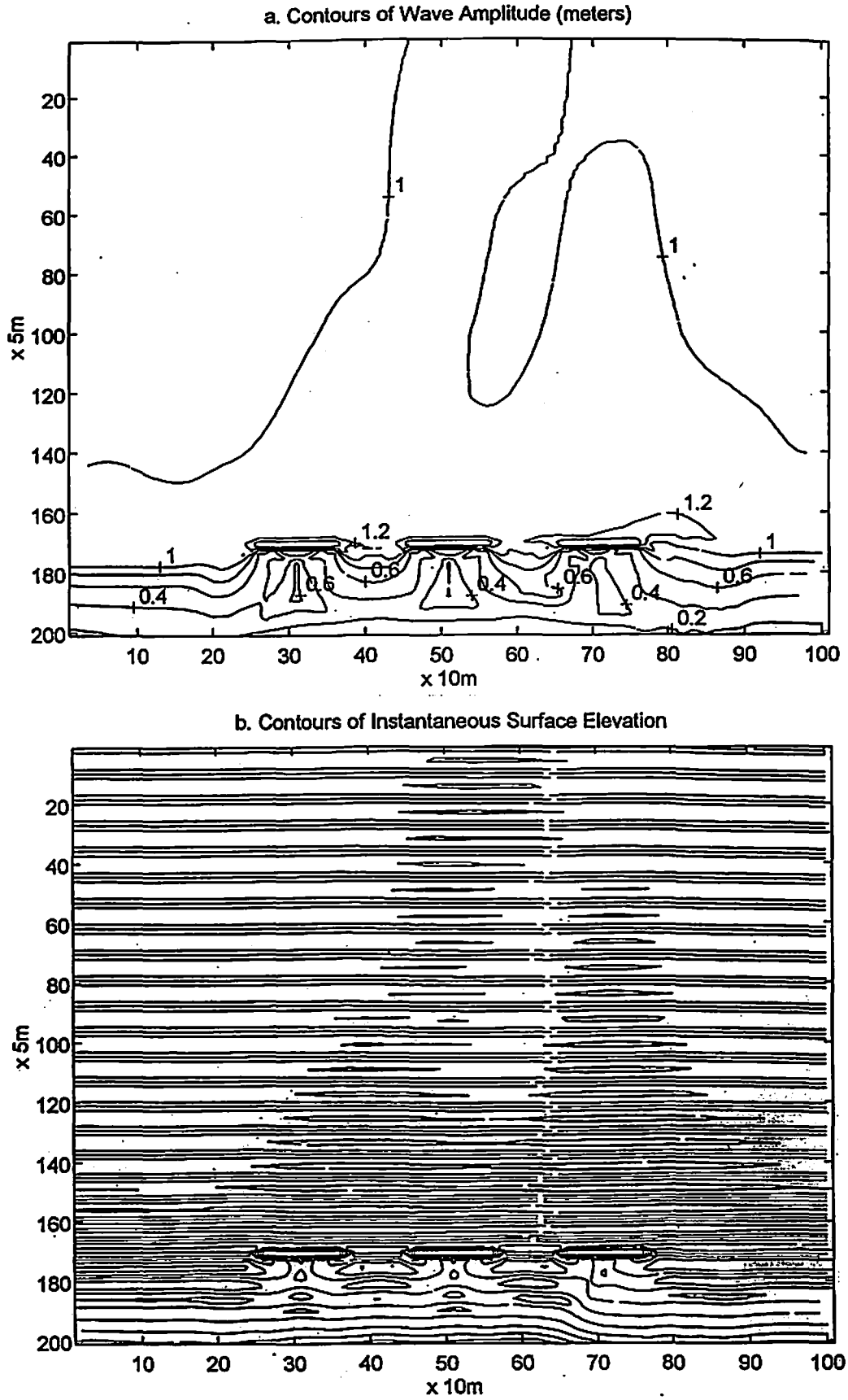

Figure 12. Wave propagation past three surface breakwaters 150 m from shore using a modal storm wave with A = 1.0 m, T = 10.0 s, D = 0°.

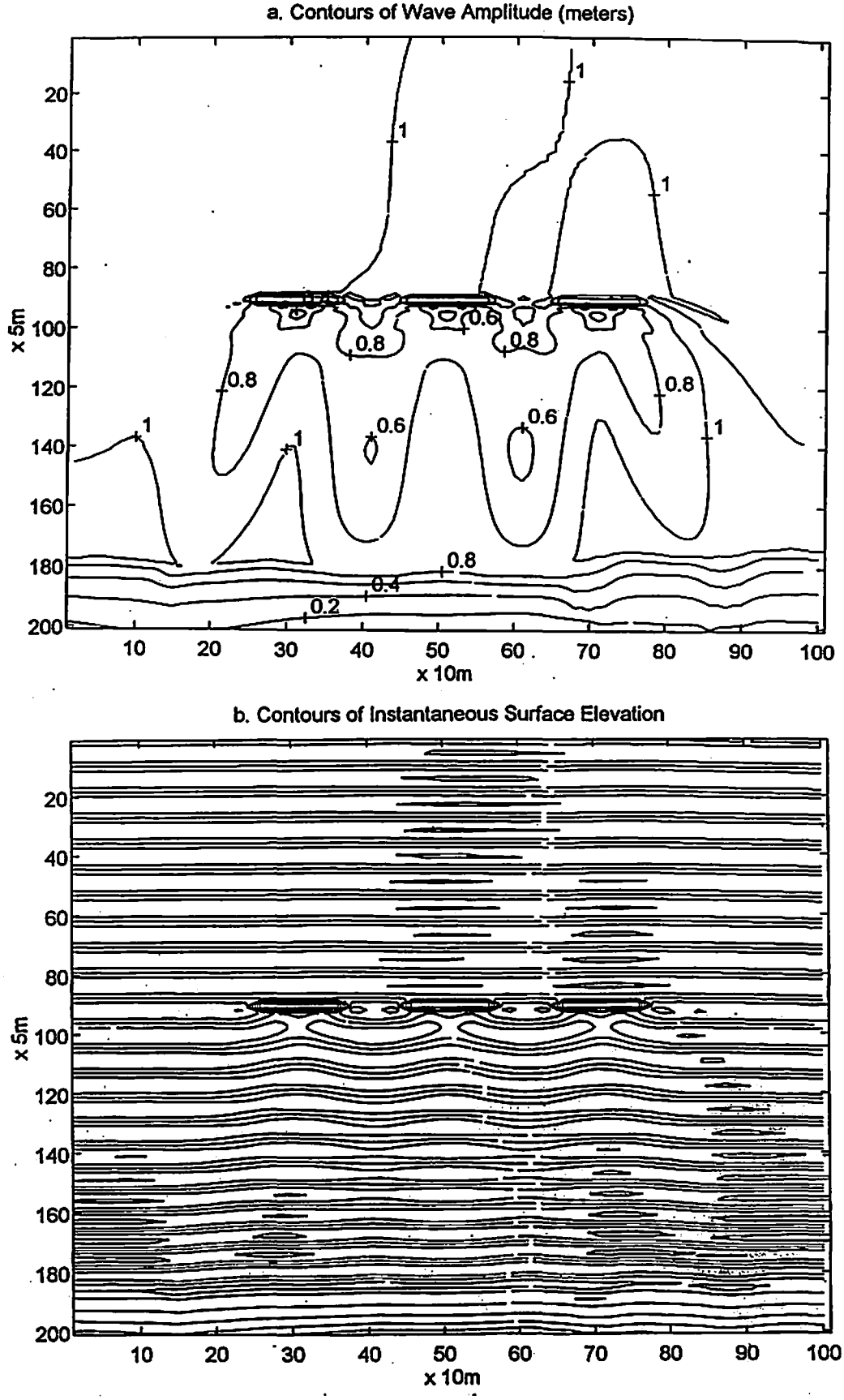

Figure 13. Wave propagation past three submerged breakwaters 550 m from shore using a modal storm wave with A = 1.0 m, T = 10.0 s, D = 0°.

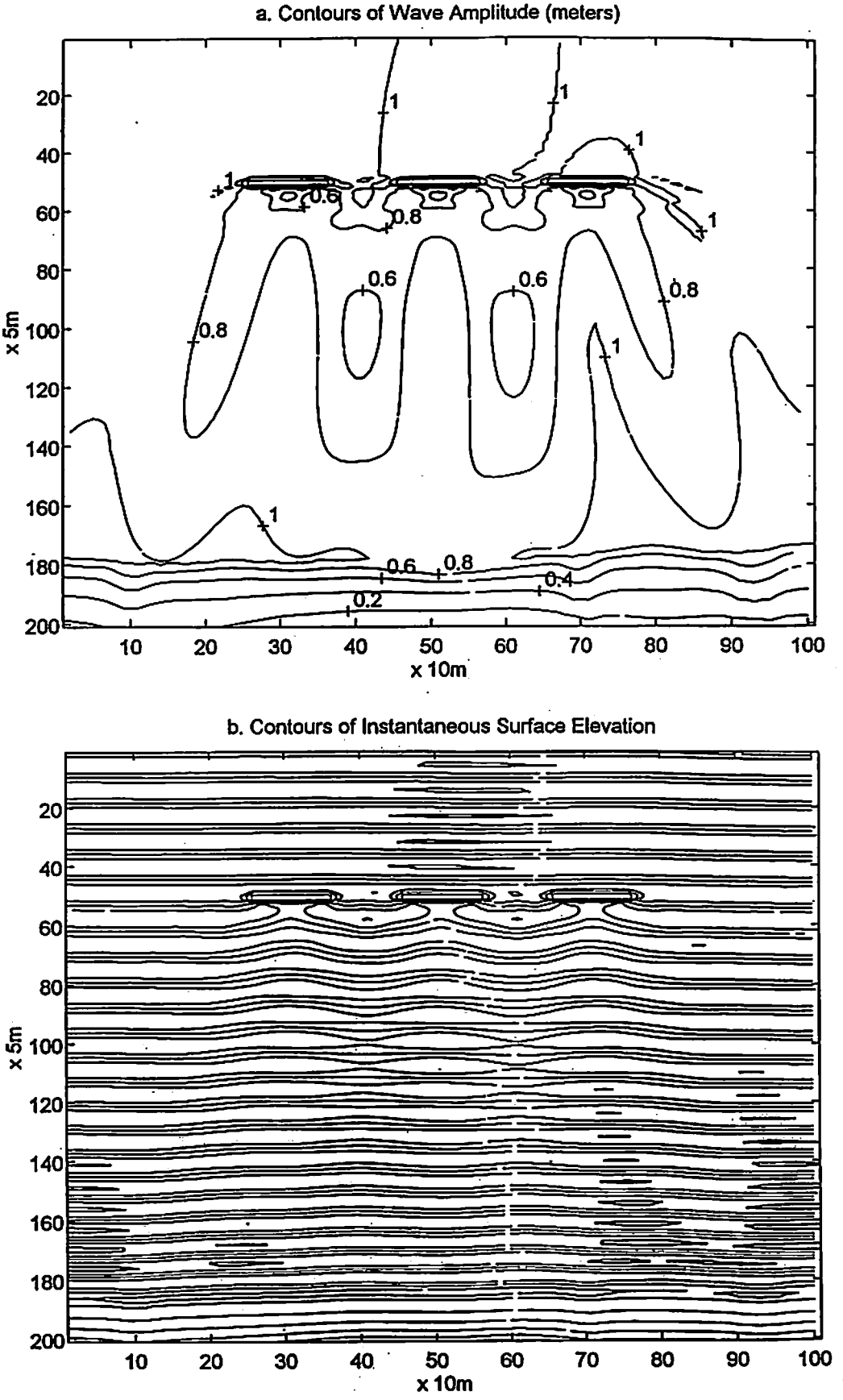

Figure 14. Wave propagation past three submerged breakwaters 750 m from shore using a modal storm wave with A = 1.0 m, T = 10.0 s, D = 0°.

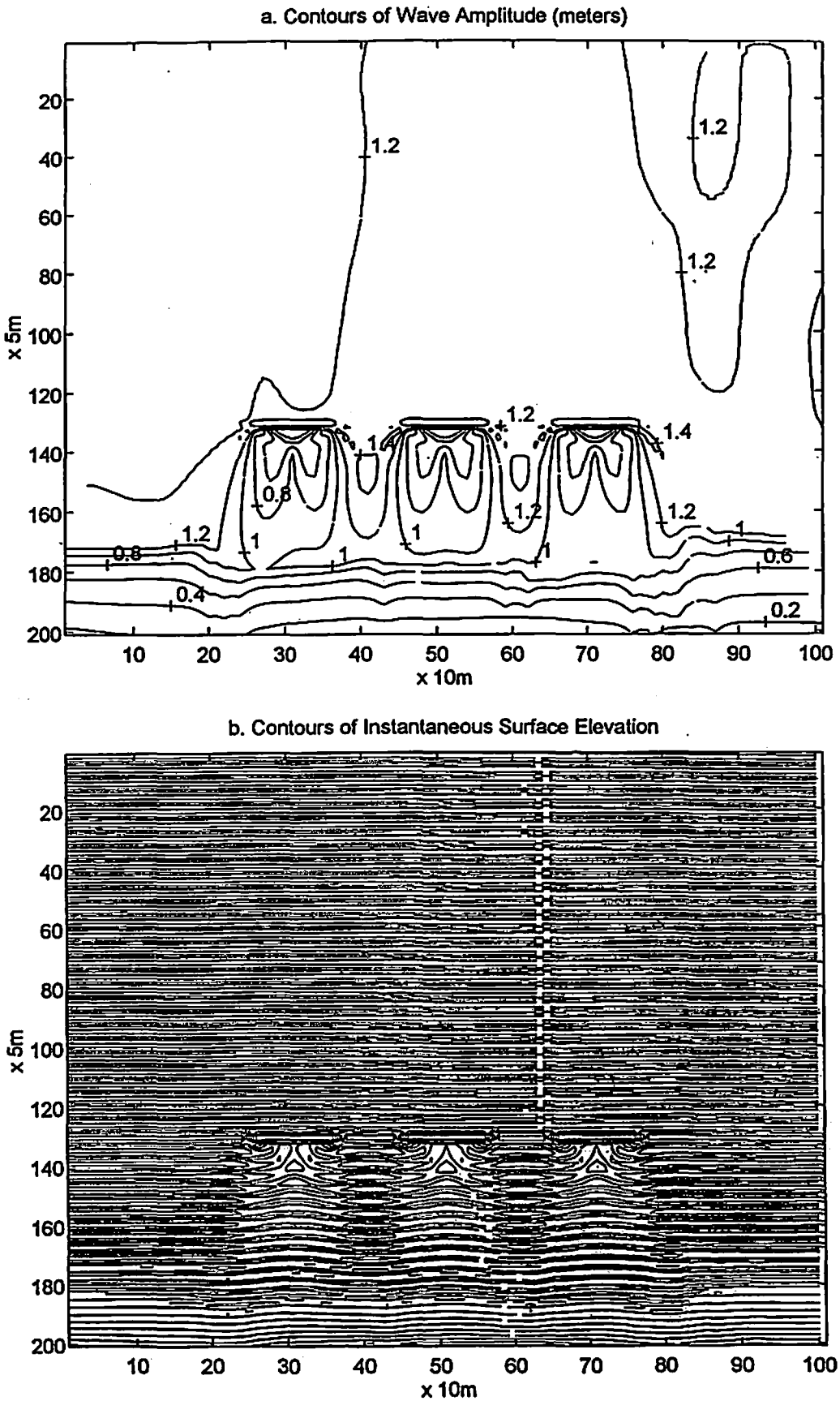

Figure 15. Wave propagation past three surface breakwaters 350 m from shore using a class extreme wave with A = 1.3 m, T = 6.0 s, D = 0°.

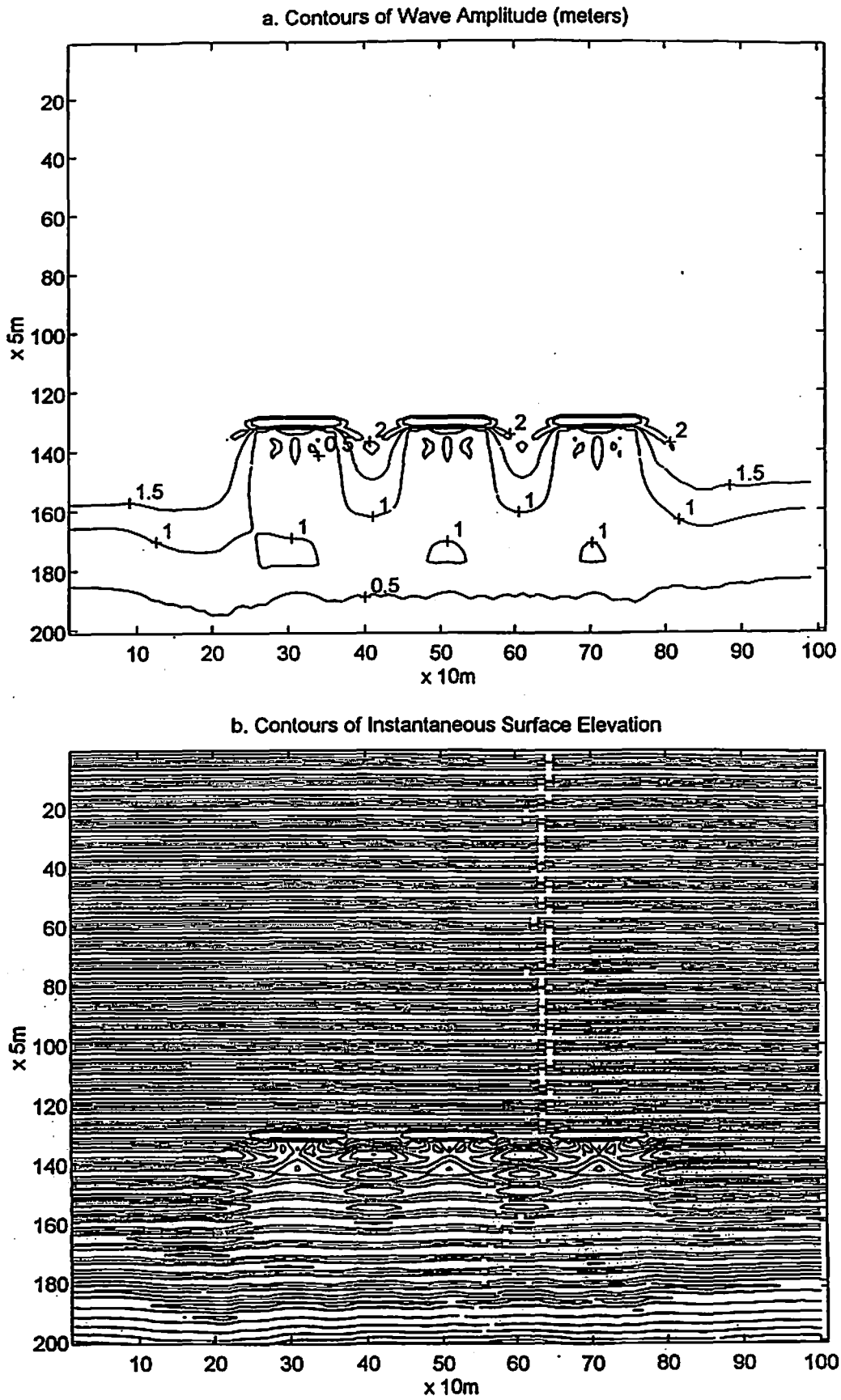

Figure 16. Wave propagation past three surface breakwaters 350 m from shore using a class extreme wave with A = 1.9 m, T = 8.0 s, D = 0°.

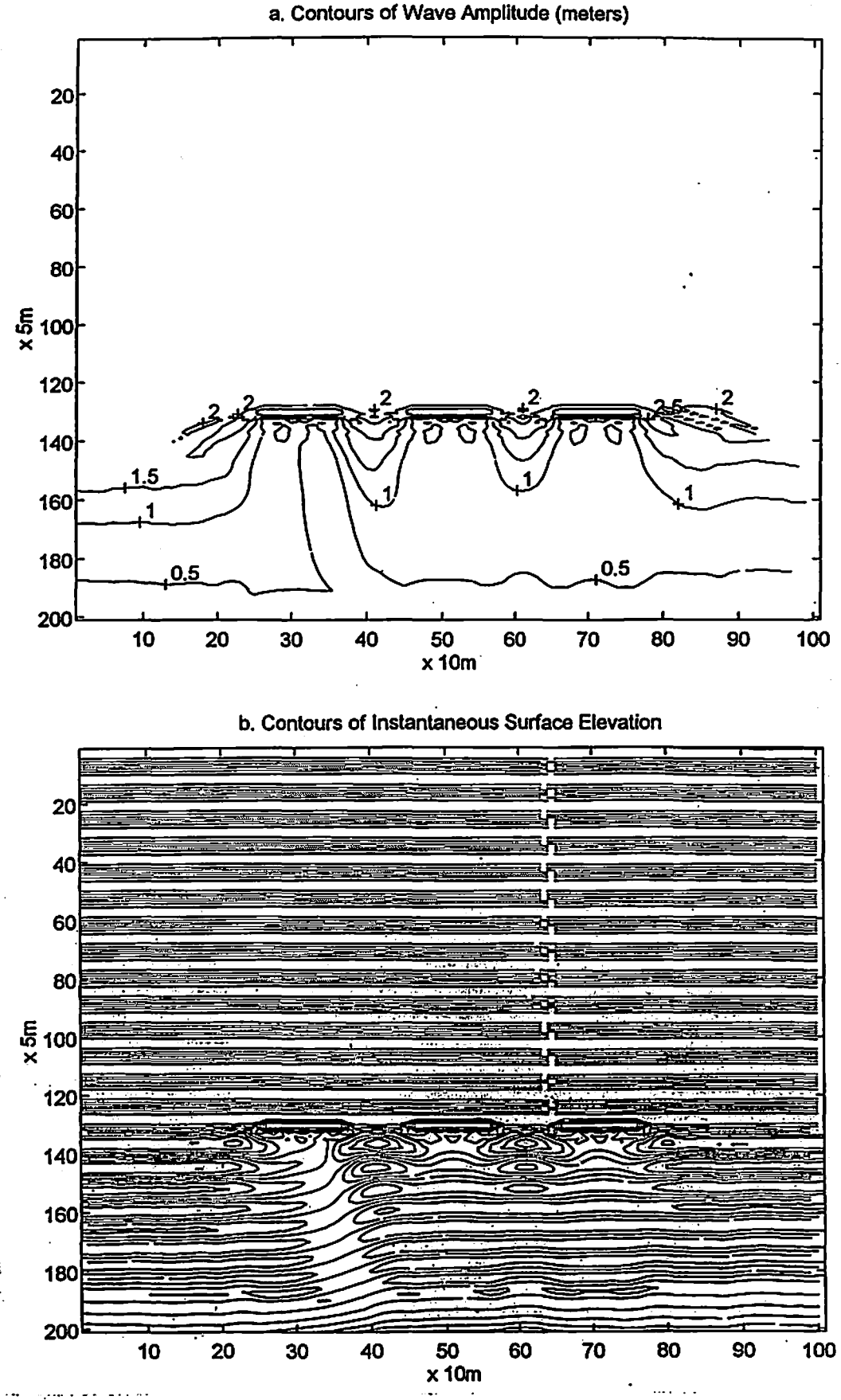

Figure 17. Wave propagation past three surface breakwaters 350 m from shore using a class extreme wave with A = 2.1 m, T = 10.0 s, D = 0°.

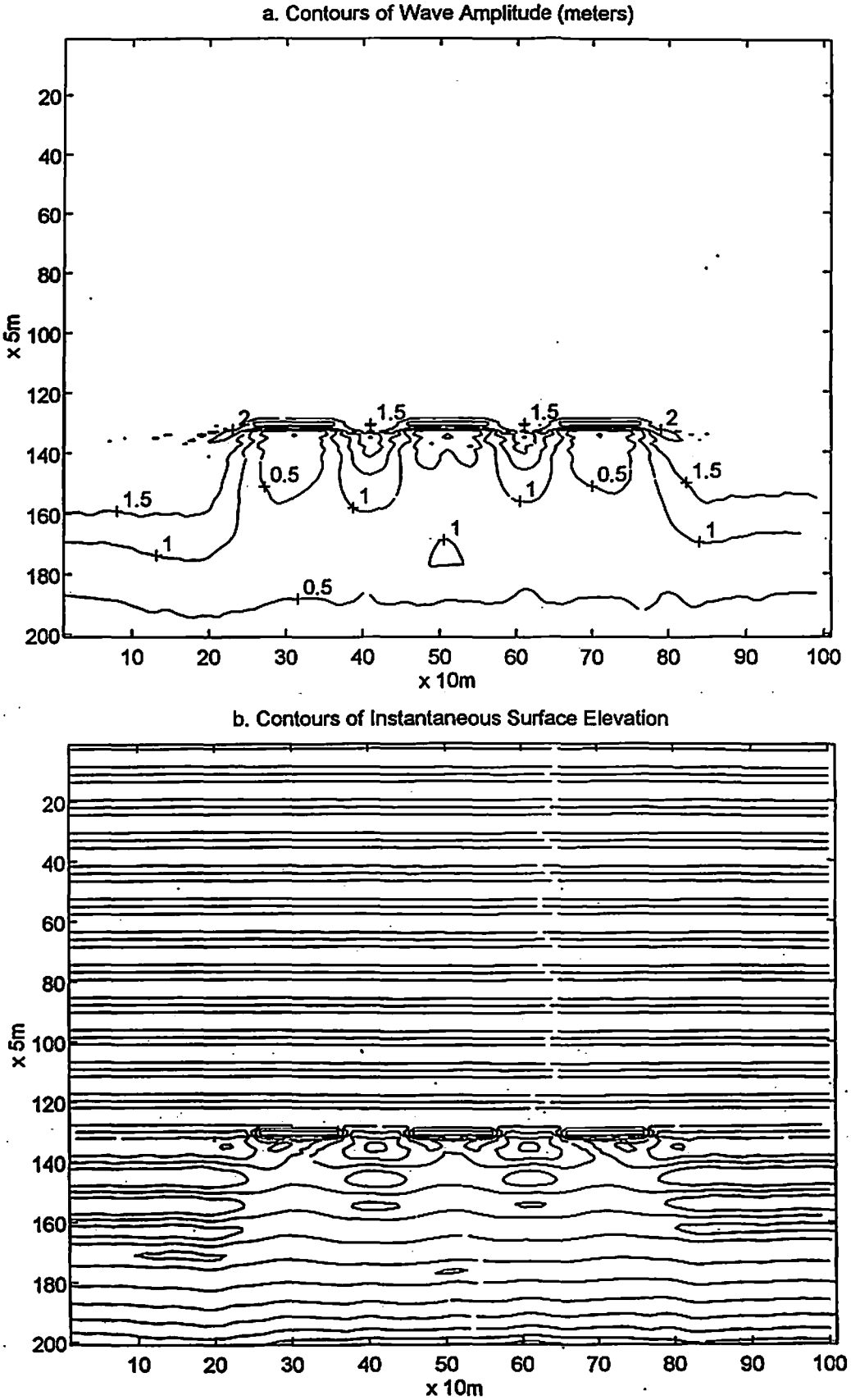

Figure 18. Wave propagation past three surface breakwaters 350 m from shore using a class extreme wave with A = 1.7 m, T = 12.0 s, D = 0°.

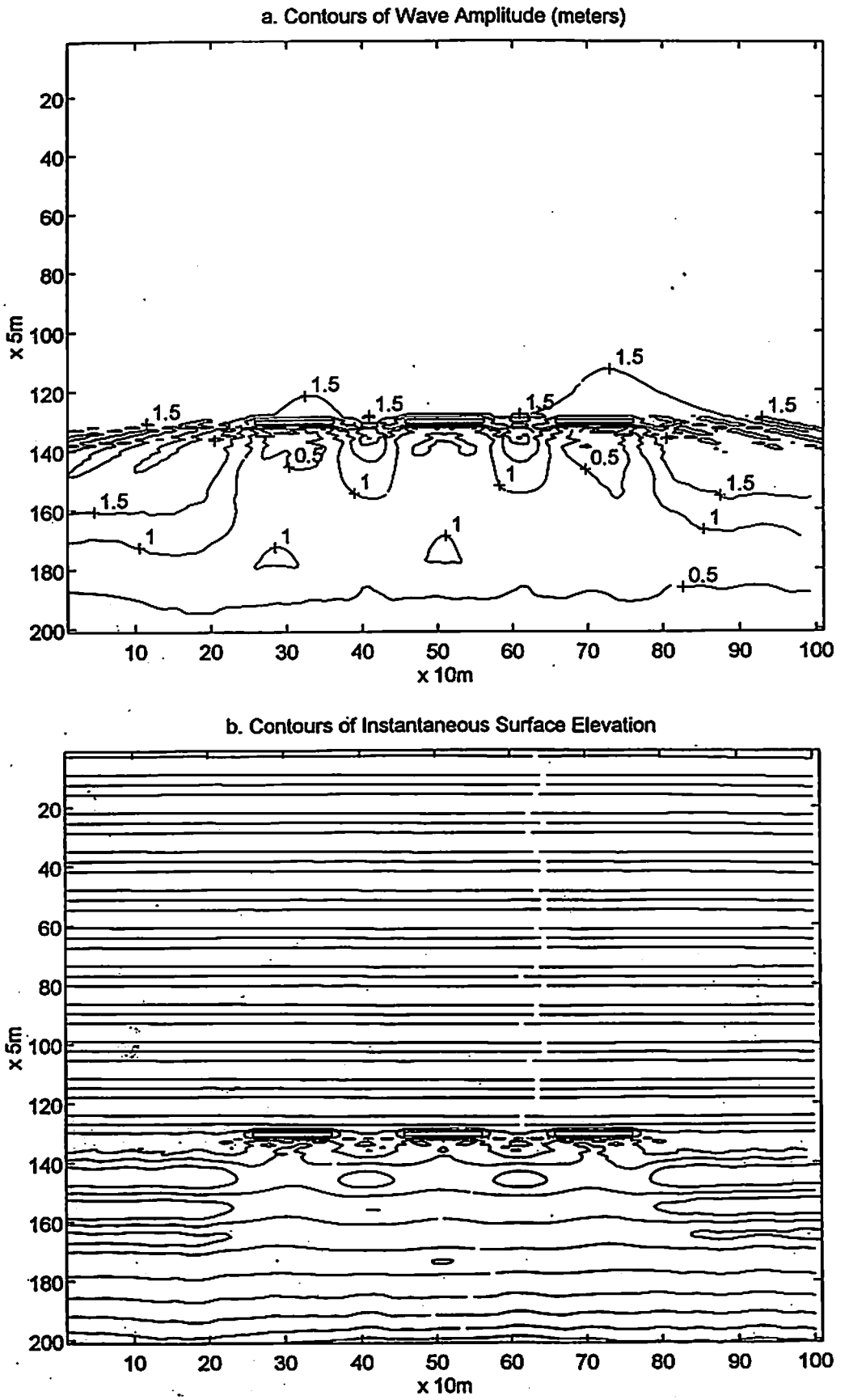

Figure 19. Wave propagation past three surface breakwaters 350 m from shore using a class extreme wave with A = 1.5 m, T = 14.0 s, D = 0°.

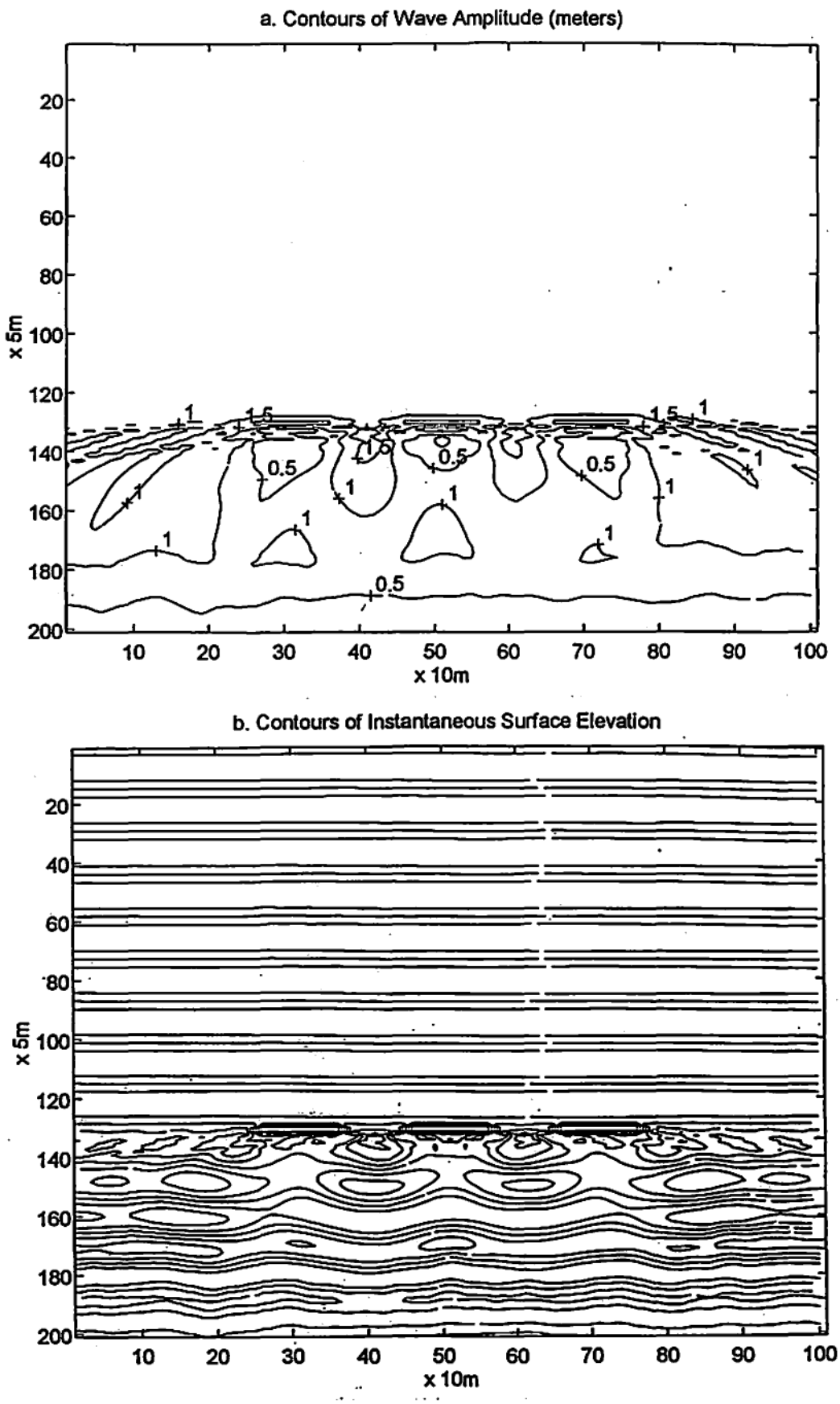

Figure 20. Wave propagation past three surface breakwaters 350 m from shore using a class extreme wave with A = 0.9 m, T = 16.0 s, D = 0°.

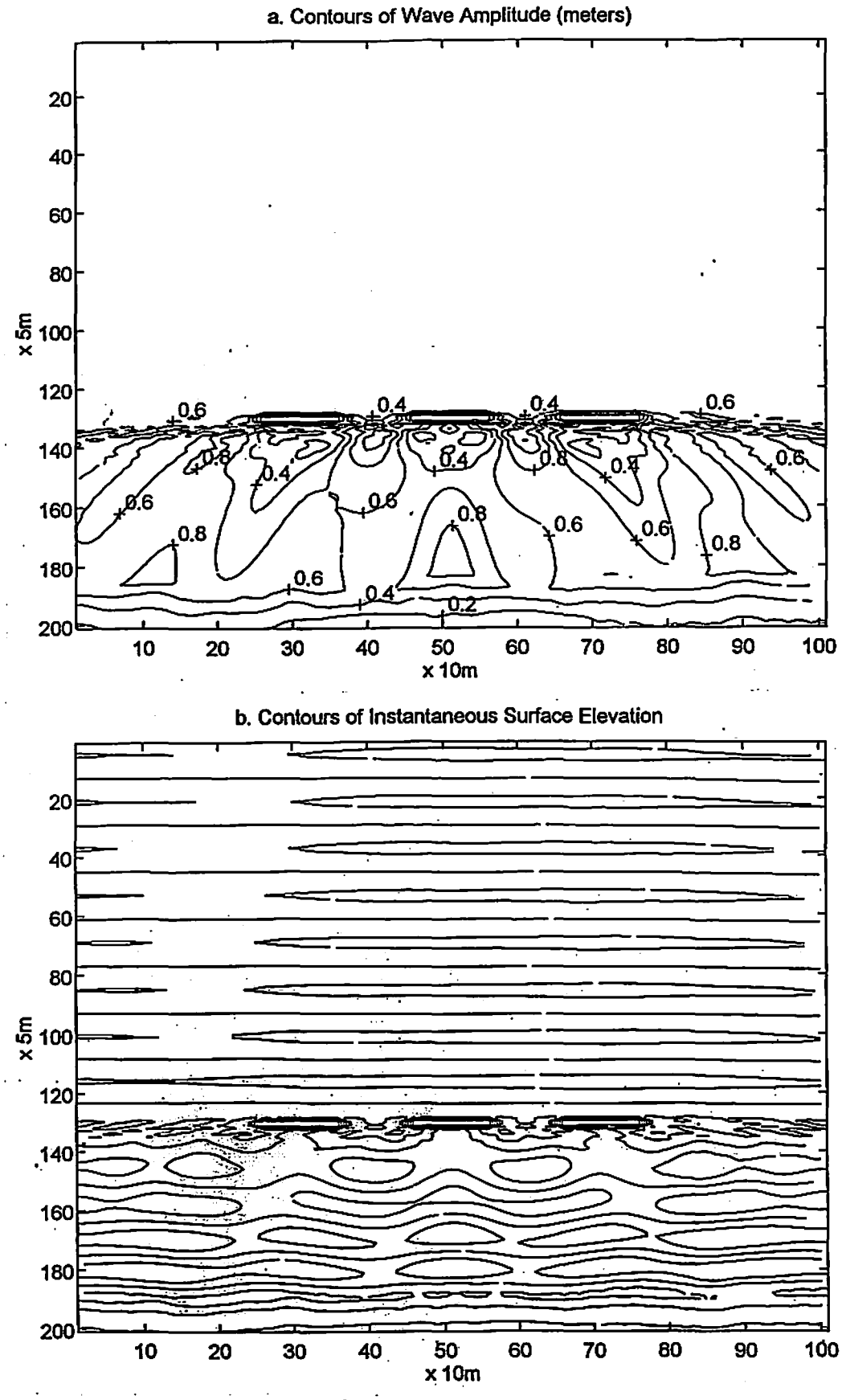

Figure 21. Wave propagation past three surface breakwaters 350 m from shore using a class extreme wave with A = 0.5 m, T = 18.0 s, D = 0°.

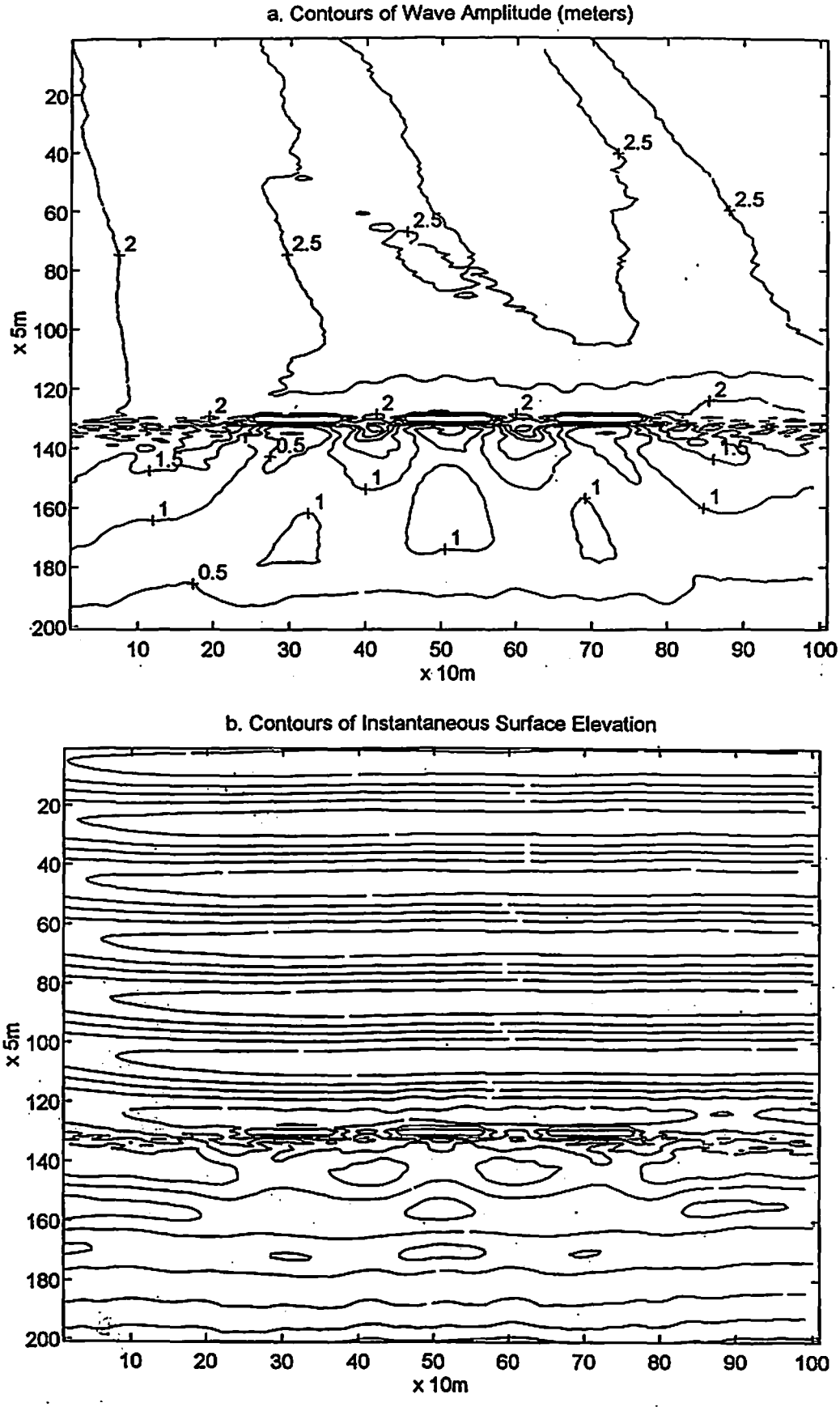

Figure 22. Wave propagation past three surface breakwaters 350 m from shore using extreme wave of record with A = 3.0 m, T = 20.0 s, D = 0°.

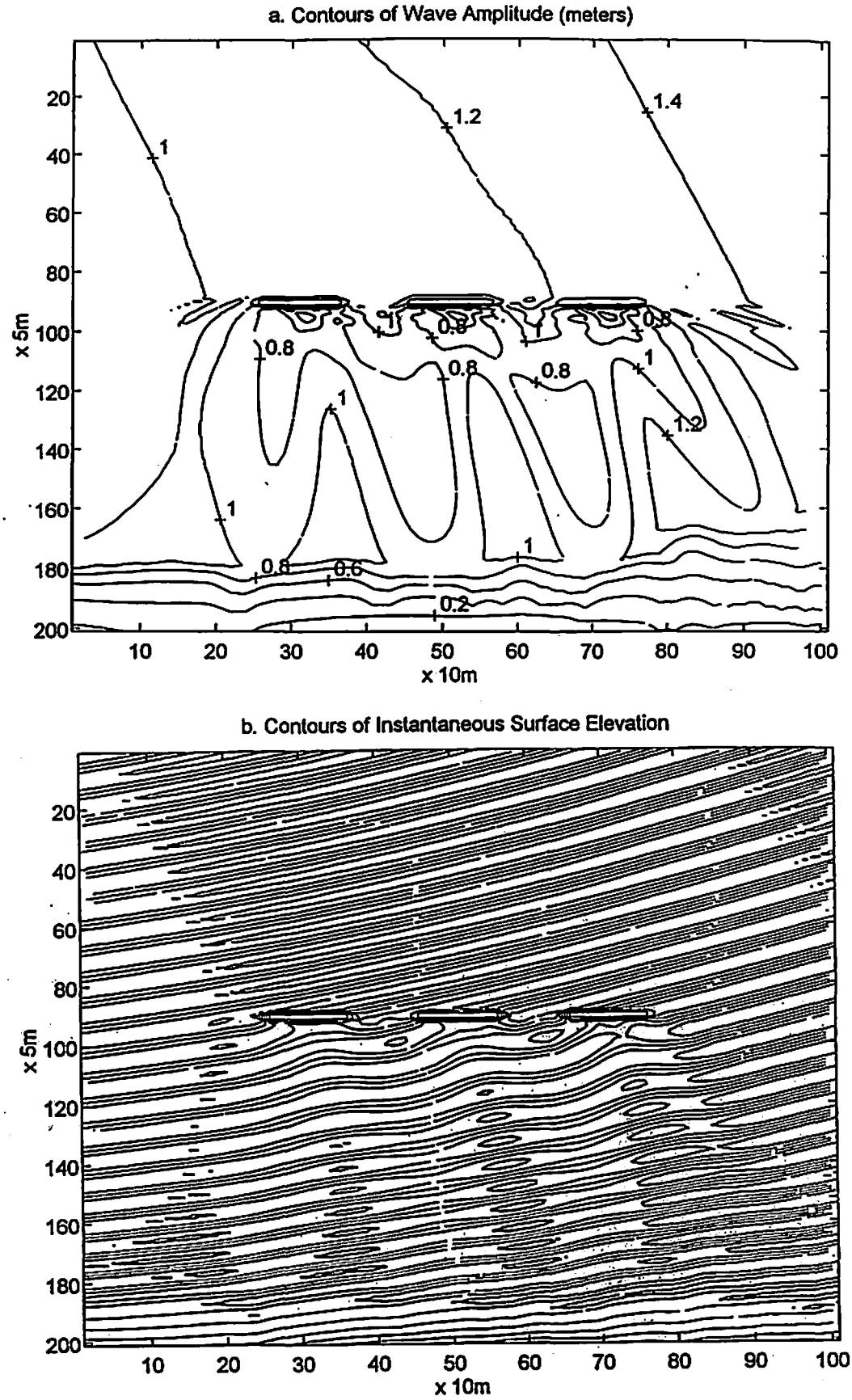

Figure 23. Wave propagation past three submerged breakwaters 550 m from shore using a class extreme wave with A = 2.1 m, T = 10.0 s, D = +30°.

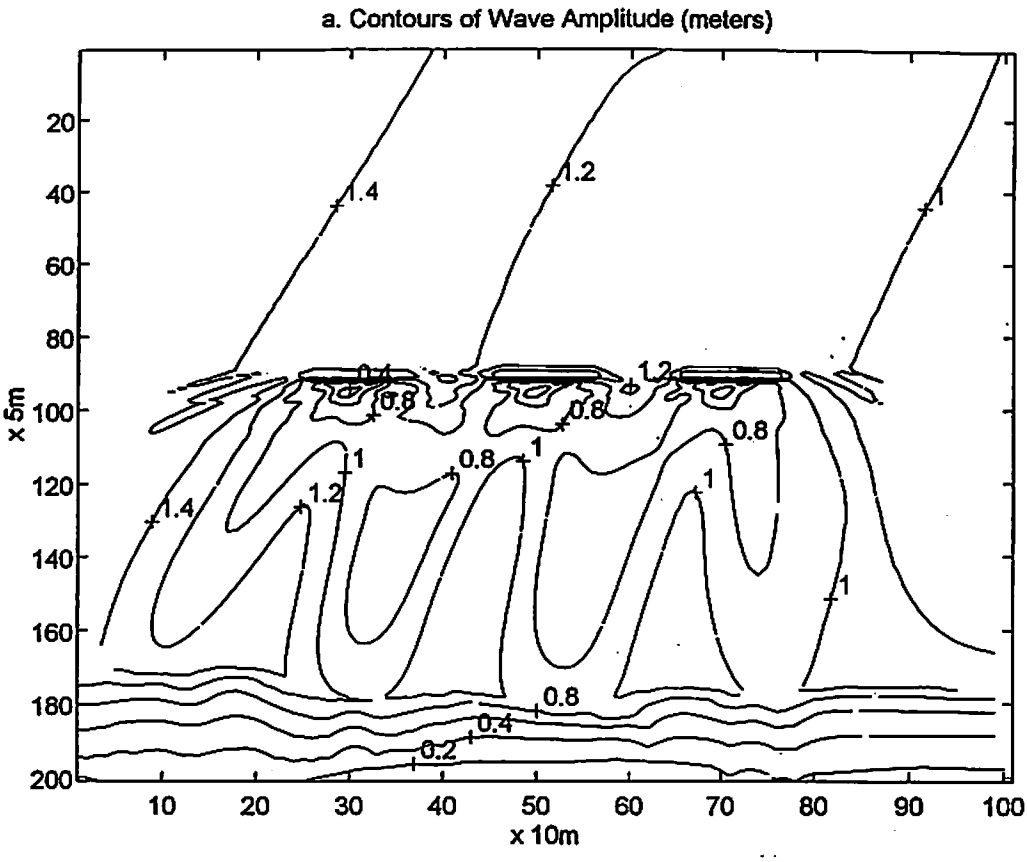

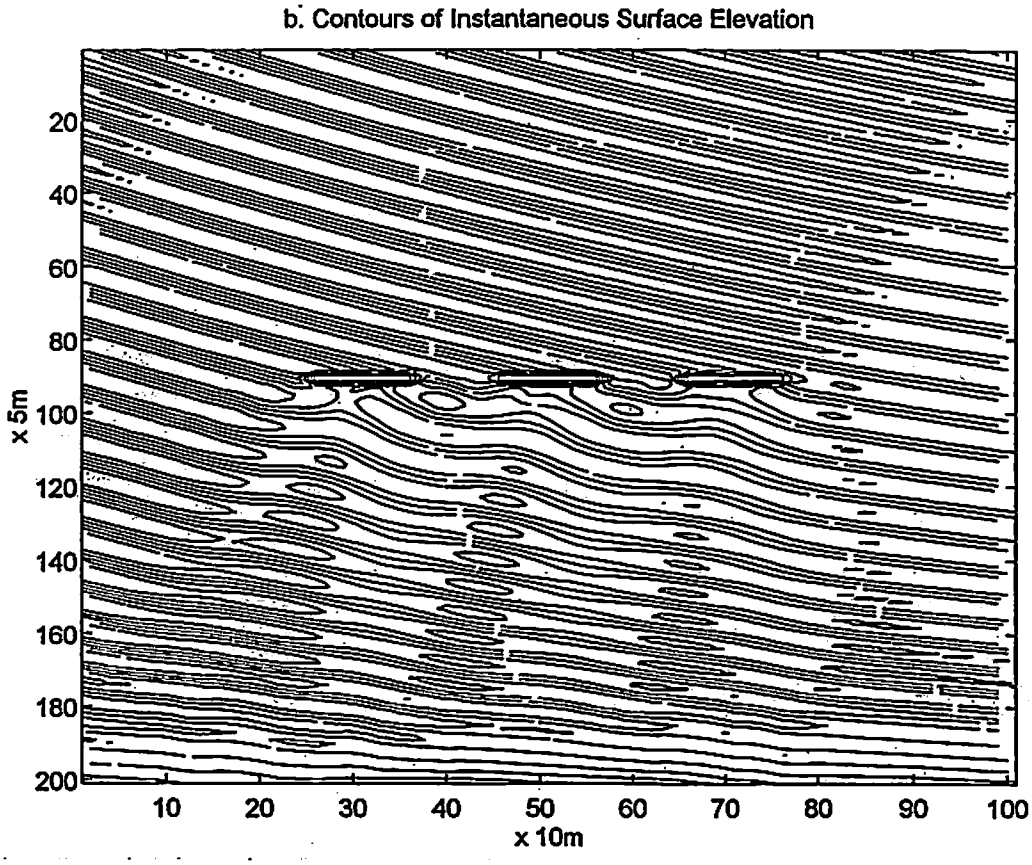

Figure 24. Wave propagation past three submerged breakwaters 550 m from shore using a class extreme wave with A = 2.1 m, T = 10.0 s, D = -30°.

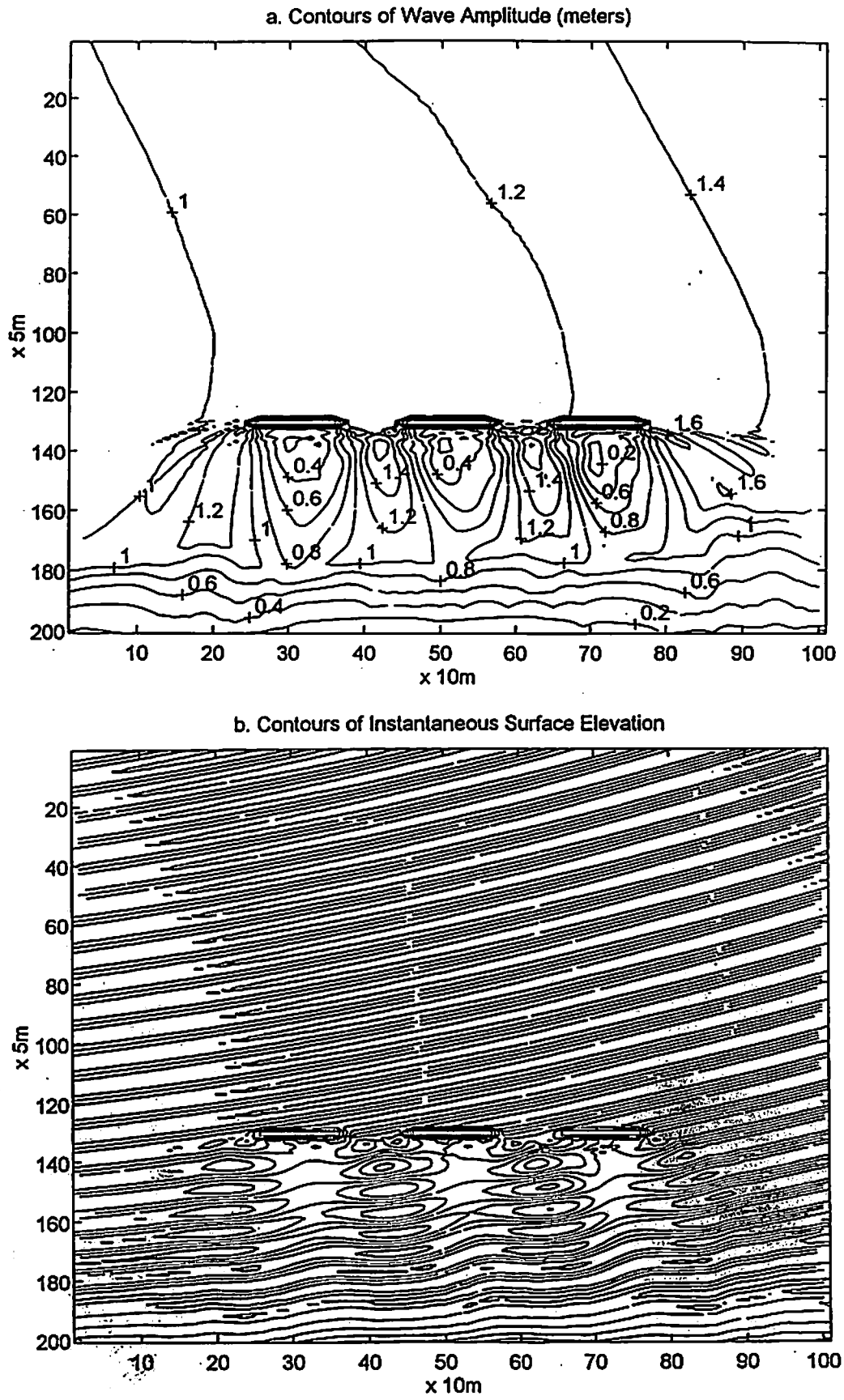

Figure 25. Wave propagation past three surface breakwaters 350 m from shore using a class extreme wave with A = 2.1 m, T = 10.0 s, D = +30°.

III. SUMMARY COMMENTS AND RECOMMENDATIONS

The **REF/DIF 1** combined refraction/diffraction wave model is an ideal tool for exploring the effects of wave interaction with structures designed to protect or enhance shoreline developments. Its unique subgrid feature permits the necessary transition from incident wave representation on a regional scale (kilometers) to a local grid fine enough to depict structural features on a scale of meters. This capability was fully required for the representation of detached breakwaters at this scale in order to evaluate their function and potential use for shore protection, which was the main goal of the study.

Application of the model to the Virginia Beach coastal sector was accomplished with little difficulty given the straightforward bathymetry and the quantity of nearshore bathymetric data available for this location. The model runs presented in this report should be regarded as preliminary, however, for several reasons. One reason has to do with the broad range of features and options available to users of the **REF/DIF 1** model. These options range from boundary layer specifications controlling the type of wave damping to wave climate (directional spectra) and current representations in the model domain. A first-order approach was adopted in this study that involved monochromatic waves of a single initial direction propagating through a motionless water column. In addition, a great many design configurations are possible using detached breakwaters. Only a few were investigated in the present study using the following concepts for guidance.

Empirical evidence suggests that detached breakwaters may function in one of two ways depending on their design characteristics:

Detached breakwaters inducing shoreline response. These are likely to be segmented breakwaters located inshore a short distance from the existing shoreline. Their structure-to-distance ratio will govern whether they induce a partial response through shoreline salient formation (low ratio) or a full response indicated by tombolo formation (high ratio). Coastlines experiencing moderate to high rates of longshore sand transport would normally employ a design of this type configured to either partially or completely inhibit such transport.

Detached breakwaters inducing nearshore response. Coastlines that experience significant offshore sand loss may not respond well to breakwaters placed too close to shore, unless the latter are constructed more or less as continuous sediment dams to prevent this loss. However, sediment mobilized during a storm is indeed lost once it has bypassed a structure of that type. Detached breakwaters placed farther from shore may incorporate configurations designed to create zones of reduced wave amplitude, or wave energy gradients, that induce sand accumulation in the intervening nearshore region. This concept recognizes that the zone of volumetric change is not limited to the subaerial beach but extends within and beyond the surf zone.

The present study offers the following observations based on model results obtained for the Virginia Beach grid using a group of three detached breakwaters:

1. Detached surface breakwaters placed 150 m or less from shore are likely to induce tombolo formation. Although wave amplitude reduction is predicted in the lee of the structures, offshore sand bypassing remains possible via the breakwater gaps at 3 m depths.

2. Detached breakwaters located 250 m to 350 m from shore should produce well-developed wave diffraction patterns that would favor salient formation at the shoreline. The choice of either a surface (0 m) or a submerged (-1 m) breakwater crest may be critical to the resulting spatial distribution of wave amplitudes landward of the structures. In the case of a submerged breakwater group, wave amplitude reduction is less overall with low amplitudes occurring in line with the breakwater gaps. In the case of a surface breakwater group, the highest wave amplitudes occur down-wave in line with the breakwater gaps and within the zones adjacent to the ends of the left and right breakwater.

3. Detached submerged breakwaters located 550 m to 750 m from shore appear unlikely to produce wave diffraction effects inshore that could initiate salient formation. A limited number of model runs suggest that wave amplitude reductions of 20% - 40% could be induced within critical nearshore areas during a modal storm event. The areas of maximum reduction are predicted to occur in discrete, shore-normal bands positioned in line with the breakwater gaps. Additional runs using different relative wave directions starting 5 km from shore predict only a small amount of lateral shifting in the position of these bands, an indication that this function of the breakwater is not direction sensitive.

4. Detached surface breakwaters located 350 m from shore show a varied response to the largest waves expected for a range of wave periods based on local wave observations (Virginia Beach offshore region, Chesapeake Light Tower). Waves in this category with periods of 10 s or less produce coherent diffraction patterns landward of the structures while waves with periods greater than 10 s do not. The maximum storm wave tested with the model (3.0 m amplitude, 20.0 s period offshore) yielded a prediction of uniform wave breaking along the extended breakwater line situated at 350 m. Lesser wave amplitudes occur inshore due to breaking.

Further testing with the REF/DIF 1 model is needed to evaluate an expanded set of breakwater configurations involving structures of varying lengths, crest heights and gap distances. Additional work in the Virginia Beach sector should focus on the feasibility of achieving a dual function with detached breakwaters, namely the creation of reduced amplitude zones inshore while simultaneously promoting salient formation (but not tombolo development) at the shoreline. A set of discrete directional waves or a simulated directional wave spectrum should be employed in these tests.

IV. REFERENCES

Ahrens, J.P., 1987. Reef Breakwater Response to Wave Attack. In "Berm Breakwaters: Unconventional Rubble-Mound Breakwaters", ASCE Hydraulics Workshop, Canada National Research Council.

CERC, 1984. Shore Protection Manual, 4th Ed. U.S. Army Engineers Waterways Experiment Station, Coastal Engineering Research Center, Vicksburg, MS.

Dalrymple, R.A. and J.T. Kirby, 1991. Documentation Manual, Combined Refraction/Diffraction Model REF/DIF 1, Version 2.3. CACR report No. 91-2, Center for Applied Research, Dept. of Civil Engineering, Univ. of Delaware, Newark, 88p.

Dally, W.R. and J. Pope, 1986. Detached Breakwaters for Shore Protection. Tech. Report CERC-86-1, U.S. Army Engineers Waterways Experiment Station, Coastal Engineering Research Center, Vicksburg, MS.

Davis, J.C., 1986. Statistics and Data Analysis in Geology, 2nd Ed. John Wiley & Sons, New York, 646p.

Dean, R.G. and R.A. Dalrymple, 1984. Water Wave Mechanics for Engineers and Scientists. Prentice-Hall, Inc., Inglewood Cliffs, New Jersey, 353p.

Ebersole, B.A., M.A. Cialone and M.D. Prater, 1986. Regional Coastal Processes Modeling system, Report 1, RCPWAVE - a Linear Wave Propagation Model for Engineering Use. Tech. Report CERC-86-4, U.S. Army Engineers Waterways Experiment Station, Coastal Engineering Research Center, Vicksburg, MS.

Hardaway, C.S., Jr. and J.R. Gunn, 1991. Headland Breakwaters in the Chesapeake Bay. ASCE, Proceedings, 7th Symposium on Coastal and Ocean Management, pp. 1267-1281.

Hardaway, C.S., Jr., J.R. Gunn and R.N. Reynolds, 1993. Breakwater Design in the Chesapeake Bay: Dealing with the End Effects. ASCE, Proceedings, 8th Symposium on Coastal and Ocean Management, pp. 27-41.

Ludwick, J.C., P. Fleischer, R.E. Johnson, and G.L. Shideler, 1975. Field Performance of Permeable Breakwater. ASCE, J. of Waterways Harbors and Coastal Engineering Div., WW4, pp. 357-368.

Rosati, J.D., 1990. Functional Design of Breakwaters for Shore Protection: Empirical Methods. Tech. Report CERC-90-15, U.S. Army Engineers Waterways Experiment Station, Coastal Engineering Research Center, Vicksburg, MS.

Suh, K.D. and R.A. Dalrymple, 1987. Offshore Breakwaters in Laboratory and Field. ASCE, J. of Waterway, Port, Coastal, and Ocean Engineering, 113:2, pp. 105-121.

Wright, L.D., C.S. Kim, C.S. Hardaway, S.M. Kimball, and M.O. Green, 1987. Shoreface and Beach Dynamics of the Coastal Region from Cape Henry to False Cape, Virginia. VIMS Contract Report to the Virginia Dept. of Conservation and Historic Resources, 116p.